BOREAS An international journal of Quaternary research

Middle to Late Pleistocene environments based on stable organic carbon and nitrogen isotopes of loess-palaeosol sequences from the Carpathian Basin

STEPHAN PÖTTER, ARNDT SCHMITZ, ANDREAS LÜCKE, PHILIPP SCHULTE, IGOR OBREHT, MICHAEL ZECH, HOLGER WISSEL, SLOBODAN B. MARKOVIĆ AND FRANK LEHMKUHL

BOREAS

Pötter, S., Schmitz, A., Lücke, A., Schulte, P., Obreht, I., Zech, M., Wissel, H., Marković, S. B. & Lehmkuhl, F.: Middle to Late Pleistocene environments based on stable organic carbon and nitrogen isotopes of loess-palaeosol sequences from the Carpathian Basin. *Boreas*. https://doi.org/10.1111/bor.12470. ISSN 0300-9483.

Stable organic carbon and nitrogen isotopes can be used to interpret past vegetation patterns and ecosystem qualities. Here we present these proxies for two loess-palaeosol sequences from the southern Carpathian Basin to reconstruct the palaeoenvironment during the past 350 ka and establish regional commonalities and differences. Before now, isotopic studies on loess sequences from this region were only conducted on deposits from the last glacial cycle. We conducted methodological tests involving the complete decalcification of the samples prior to stable isotope analyses. Two decalcification methods (fumigation method and wet chemical acidification), different treatment times, and the reproducibility of carbon isotope analyses were tested. Obtained results indicate that the choice of the decalcification method is important for organic carbon stable isotope analyses of loess-palaeosol sequences because ratios vary by more than 10‰ between the wet chemical and fumigation methods, due to incomplete carbonate removal by the latter. Therefore, we suggest avoiding the fumigation method for studies on loess-palaeosol sequences. In addition, our data show that samples with TOC content <0.2% bear increased potential for misinterpretation of their carbon isotope ratios. For our sites, C_3-vegetation is predominant and no palaeoenvironmental shifts leading to a change of the dominant photosynthesis pathway can be detected during the Middle to Late Pleistocene. Furthermore, the importance of further stable nitrogen isotope studies is highlighted, since this proxy seems to reflect past precipitation patterns and reveals favourable conditions in the southern Carpathian Basin, especially during interstadials.

Stephan Pötter (stephan.poetter@geo.rwth-aachen.de), Arndt Schmitz, Philipp Schulte and Frank Lehmkuhl, Department of Geography, RWTH Aachen University, Wüllnerstraße 5b, Aachen 52064, Germany; Andreas Lücke and Holger Wissel, Institute of Bio- and Geosciences, Agrosphere (IBG-3), Forschungszentrum Jülich GmbH, Wilhelm-Johnen-Straße, Jülich 52428, Germany; Igor Obreht, Organic Geochemistry Group, MARUM-Center for Marine Environmental Sciences and Department of Geosciences, University of Bremen, Leobener Str. 8, Bremen 28359, Germany; Michael Zech, Institute of Geography, Technical University of Dresden, Helmholtzstraße 10, Dresden 01069, Germany; Slobodan B. Marković, Chair of Physical Geography, University of Novi Sad, Trg Dositeja Obradovića 3, Novi Sad 21000, Serbia; *received 16th April 2020, accepted 17th July 2020.*

Due to its widespread distribution and its atmospheric transport, loess is a frequently used terrestrial archive for the reconstruction of past climatic conditions (Pécsi 1990; Pécsi & Richter 1996; Antoine *et al.* 2009; Zöller 2010; Muhs 2013; Rousseau *et al.* 2014; Sprafke & Obreht 2016; Obreht *et al.* 2017). During the last decades of research, a multitude of proxy data approaches for palaeoclimate reconstruction in loess research have been developed (e.g. Zech *et al.* 2010; Jia *et al.* 2013; Beck *et al.* 2018). Some of these approaches use the physical and (in-)organic chemical properties of sediment samples as proxies for sedimentation dynamics, as well as syn- and postdepositional alteration processes (Buggle *et al.* 2011; Schaetzl *et al.* 2018; Schulte & Lehmkuhl 2018; Schulte *et al.* 2018), ultimately aiming to reconstruct palaeoclimatic fluctuations (Heller & Tungsheng 1986; Gallet *et al.* 1996; Lu & An 1998; Antoine *et al.* 2009; Torre *et al.* 2020). Another approach is to investigate the remnants of organic material within the sediment. Since macroscopic plant remnants are rare in loess deposits (Zech *et al.* 2013), methods from organic geochemistry are applied at molecular or isotopic scales (Lin *et al.* 1991; Hatté *et al.* 1998, 1999; Schatz *et al.* 2011).

Stable organic carbon isotopes ($\delta^{13}C_{org}$) are investigated to draw conclusions about the dominant pathway of photosynthesis of the palaeovegetation. C_4 plants, which are favoured under warm and arid conditions (Lin *et al.* 1991; Wang *et al.* 1997; Rao *et al.* 2013), tend to have less negative ratios of around −9 to −15‰. On the contrary, C_3 plants, which grow under cooler, more humid climatic conditions, have more depleted $\delta^{13}C_{org}$ ratios of around −20 to −38‰ (O'Leary 1988; Farquhar *et al.* 1989). In aeolian sediments, stable organic carbon isotopes have been investigated since the early 1990s. Pioneering studies were conducted in China (Lin *et al.* 1991; Tungsheng *et al.* 1996; Wang *et al.* 1997; Gu *et al.* 2003). Hatté *et al.* (1998, 1999, 2001) intensively investigated the isotopic signatures of loess-palaeosol sequences (LPS) in the Upper Rhine Graben and the Neckar basin in southwestern Germany as well as in eastern France, where carbon isotope ratios were also

DOI 10.1111/bor.12470

used to reconstruct palaeoprecipitation patterns of these regions (Hatté *et al.* 2001; Hatté & Guiot 2005). Studies were also conducted in Central Asia (Ding *et al.* 2002; Rao *et al.* 2013), Siberia (Zech *et al.* 2007) and North America (Muhs *et al.* 1999). In southeastern Europe, stable carbon isotope studies focused on LPS from the last glacial cycle in the Carpathian Basin (Schatz *et al.* 2011; Hatté *et al.* 2013; Zech *et al.* 2013; Obreht *et al.* 2014; Marković *et al.* 2018).

Since other carbon sources in LPS, especially carbonates, are considerably enriched in $\delta^{13}C$ values compared to organic matter (Cerling 1984; Han *et al.* 1997; Ding & Yang 2000; Kaakinen *et al.* 2006; Prud'homme *et al.* 2018), a complete decalcification of the samples is crucial to ensure reliable results of $\delta^{13}C_{org}$ measurements (Gauthier & Hatté 2008; Brodie *et al.* 2011). Otherwise, the isotopic signature of the organic matter is masked by enriched values from carbonates, which makes a palaeoenvironmental reconstruction impossible.

Besides $\delta^{13}C_{org}$, stable nitrogen isotopes are another proxy informative of various environmental conditions (Zech *et al.* 2007; Schatz *et al.* 2011; Andreeva *et al.* 2013; Obreht *et al.* 2014). Since nitrogen is one of the basic elements of vegetal life, the nitrogen content of soil or sediment is informative of (past) vegetation patterns (Jenny 1941; Post *et al.* 1985). During the uptake of nitrogen by plants, the abundant isotopes of nitrogen, ^{14}N and ^{15}N are fractionated, due to the favoured uptake of the lighter ^{14}N (Robinson 2001). The resulting nitrogen isotope ratio ($\delta^{15}N$) is mostly interpreted as a proxy of the characteristics of the biogeochemical nitrogen cycle (Amundson *et al.* 2003; Obreht *et al.* 2019). Characteristics of the nitrogen cycles, in particular openness and closeness, are determined by e.g. the input and losses of nitrogen within an ecosystem (Amundson *et al.* 2003). A significant input or severe losses of nitrogen within a system opens the nitrogen cycle, leading to an increase of the $\delta^{15}N$ ratio (Zech *et al.* 2011). There are also studies on the linkage of $\delta^{15}N$ to (palaeo-)climatic parameters such as precipitation or temperature (Aranibar *et al.* 2004; Terwilliger *et al.* 2008; Schatz *et al.* 2011). Despite its wide application in recent ecological studies of plant-soil systems (Delwiche & Steyn 1970; Evans 2001; Aranibar *et al.* 2004; Szpak 2014; Craine *et al.* 2015), palaeoenvironmental reconstructions based on the $\delta^{15}N$ ratio of LPS are still scarce (Zech *et al.* 2007, 2013; Schatz *et al.* 2011; Obreht *et al.* 2014; Liu & Liu 2017).

The Carpathian Basin is of special interest for palaeoenvironmental reconstructions based on LPS because its deposits are the thickest and most complete archives for Quaternary environmental changes in Europe (Marković *et al.* 2015; Obreht *et al.* 2019). Covering partially the last one million years, the loess deposits of the Carpathian basin bear information about the climatic and environmental fluctuations of the Early to Late Pleistocene (Marković *et al.* 2011). Due to its characteristics, the Carpathian Basin acted as a glacial refugium for flora (Willis *et al.* 2000) and fauna (Varga 2010; Wielstra *et al.* 2013). It is also supposed to be a gateway of hominids, especially anatomically modern humans, into Europe (Hauck *et al.* 2017; Chu 2018; Staubwasser *et al.* 2018). In that context, knowledge of the environmental conditions during the Pleistocene within the Carpathian Basin is fundamental.

Here we present the results of a high-resolution stable isotope study of two Middle to Late Pleistocene LPS from the Carpathian Basin, covering the last two to three glacial–interglacial cycles. Our aims are (i) to detect the commonalities and differences in two archives from central-eastern Europe, (ii) to exploit the potential for regional palaeoenvironmental inferences from a stable isotope approach, and (iii) to apply known geochemical methods based on stable carbon and nitrogen isotopes on deposits older than the last glacial cycle. In this context, we performed methodological tests on (i) the completeness of carbonate removal and (ii) on the reproducibility of $\delta^{13}C_{org}$ measurements of samples with a generic low content of organic carbon (TOC), such as typical loess. These tests are conducted to complement known methodological works and issues (Gauthier & Hatté 2008), and to expand the critical evaluation of the proxy to older loess deposits. Besides a palaeoenvironmental reconstruction for two different settings within the southern Carpathian Basin, methodological implications on past and future stable carbon isotope studies, as well as the potential of $\delta^{15}N$ as a useful proxy for qualities of (palaeo-)ecosystems are presented.

Study area and sampling sites

The Carpathian Basin subsided due to the orogenesis of the Alps, the Carpathians and the Dinarides. This subsidence favoured thick Neogene to Quaternary sediment infills. The surface geology of the Carpathian Basin is therefore dominated by sedimentary successions (Bergerat 1989; Horváth 1993; Dolton 2006). These are mainly of lacustrine (Kázmér 1990), fluvial (Gábris 1994) or aeolian origin (Ruszkiczay-Rüdiger *et al.* 2009). During the Pleistocene, large braided river and alluvial fan systems developed along the Danube and its tributaries (Gábris 1994; Lóczy 2008; Miklós & Neppel 2010; Miklánek 2012). These fluvial sediments provided major dust source areas for aeolian deflation (Smalley & Leach 1978; Buggle *et al.* 2008; Smalley *et al.* 2009; Lehmkuhl *et al.* 2018). The deflated material was deposited in the Carpathian Basin in the form of aeolian sands (Sebe *et al.* 2011, 2015; Kiss *et al.* 2012; Gavrilov *et al.* 2018) and loess (Haase *et al.* 2007; Marković *et al.* 2008, 2012; Sümegi *et al.* 2011; Sprafke 2016; Zeeden *et al.* 2016; Lehmkuhl *et al.* 2018; Bösken *et al.* 2019). The LPS of the Carpathian Basin are amongst the most complete

terrestrial archives for the Quaternary in Europe (Marković *et al.* 2015) and have been intensively studied for palaeoclimatic and palaeoenvironmental reconstructions as well as for (geo-)archaeological investigations (e.g. Marković *et al.* 2016; Bösken *et al.* 2017).

The Semlac loess sequence, located in the Arad plain in Romania in the southeastern Carpathian Basin (latitude 46°7′N, longitude 20°57′E, altitude ~100 m a.s.l., Fig. 1), is a natural outcrop on the northern bank of the Mureş river. The plain is covered with alluvial sediments and loess derivates (Lehmkuhl *et al.* 2018), which were deposited on a plateau. The recent climate is warm moderate, with a mean annual precipitation (MAP) of less than 600 mm and precipitation maxima in summer. The mean annual air temperature (MAAT) of the nearby Arad climate station is about 11 °C (climate-data.org 2019). The plateau-like deposit is 10.75 m thick and covers the last three glacial–interglacial cycles. The basal part of the section (10.75–9.95 m) is a brownish loess (L4) and shows greyish spots with rusty halos (Fig. 2). This part is intensively manganese spotted. The palaeosol above (S3) is characterized by reddish colours (9.95–9.30 m), transitioning into more brownish hues (9.30–9.05 m). Between 9.05 and 8.35 m, a layer of brown loess can be found (L3). The above lying palaeosol shows reddish-light brown shades until 7.53 m and changes to darker colours above until 6.86 m. Between 6.86 and 6.34 m, the palaeosol has a dark brown colour. This part is also influenced by secondary carbonate precipitations. The top of the palaeosol is characterized by a transitional horizon between 6.34 and 6.18 m towards the overlying loess (L2). This loess package, which reaches until 3.02 m, is characterized by varying colours and carbonate concretions. The last interglacial pedocomplex (S1) comprises a 52-cm-thick weak brown chernozem, which is followed by a 50-cm-thick dark brown chernozem. The overlying loess (L1LL2, 2.02–1.63 m) shows some crotovinas. Between 1.63 and 0.97 m, a brown loamy soil occurs (L1SS1). Above that, a layer of light brown loess adjoins (0.97–0.35 m, L1LL1), which is topped by a dark brown, slightly eroded chernozem (0.35–0 m; S0). The nomenclature of the loess and palaeosol layers of both sections is applied according to Marković *et al.* (2015). For more detailed stratigraphical information see Zeeden *et al.* (2016). The section was sampled in 2010.

The Irig section (45°05′N, 19°52′E, ~180 m a.s.l.) is exposed in a brickyard in the southern foothills of the Fruška Gora Mountains in Serbia, which are covered by a loess mantle, which thins up with increasing elevation (Marković *et al.* 2012; Lehmkuhl *et al.* 2018). It is located at the eastern bank of the Jelence creek. The nearby climate station of Belgrade shows MAP amounts of 691 mm and a MAAT of 12.5 °C (hidmet.gov.rs 2019). The lowest part of the section is dominated by a pedocomplex (S2, an equivalent of MIS 7, Fig. 2). This pedocomplex shows more brownish colours at the base and it transitions into reddish shades above. The overlying loess (L2, until 5.1 m) is characterized by a slight colour change towards lighter hues in the upper half. At a depth of around 8.20 m, a tephra layer occurs. The transition between this loess package and the overlying palaeosol (S1, 5.1–4.3 m) is sharp. The strong brown-reddish palaeosol is topped by a 1-m-thick loess layer (L1LL2). Two chernozem-like palaeosols (3.3–3.0 m: L1SS1SSS2; 2.4–2.0 m: L1SS1SSS1) are intercalated by a thin layer of loess in L1SS1LLL1. Between 2.0 and 0.45 m, porous, yellow loess is visible (L1LL1). The sequence is topped by a modern chernozem (0–0.45 m, S0). The outcrop was initially investigated by Marković *et al.* (2007) for sedimentology and malacology. The here investigated section was resampled with stratigraphical overlap in 2009 for the upper 6 m and in 2013 for the lower 4.15 m.

For the geochronology for Semlac, the reader is referred to the published luminescence-based age model by Zeeden *et al.* (2016). The age model for Irig is based on results from Marković *et al.* (2007). The model relies on four luminescence ages and the use of amino acid racemization. However, the dating was not performed on the exact same section, and we state that the time constraint is established on the glacial–interglacial scale following the stratigraphical model from Marković *et al.* (2015).

Material and methods

Sampling

At both sections, the profile wall was carefully cleaned prior to sampling to remove weathered and relocated material from the surface. While cleaning, several cm to dm, depending on the structure of the wall, were taken away. Sampling was conducted in continuous sampling trenches in 5 cm increments. The samples were taken with cleaned tools and packed in sterile plastic bags to avoid contamination. Both sections were sampled in sub-profiles with a stratigraphical overlap and were correlated by using magnetic susceptibility and grain-size data in order to obtain seamless stratigraphical columns for both sections.

Sample preparation and methodological and reproducibility tests

Since there is a multitude of methods for carbonate removal from soil and loess samples and they have a crucial impact on the elemental and isotopic signature of the samples (Gauthier & Hatté 2008; Brodie *et al.* 2011), we compared two methods: the fumigation method (FM) using silver (Ag) capsules and the wet chemical decalci-

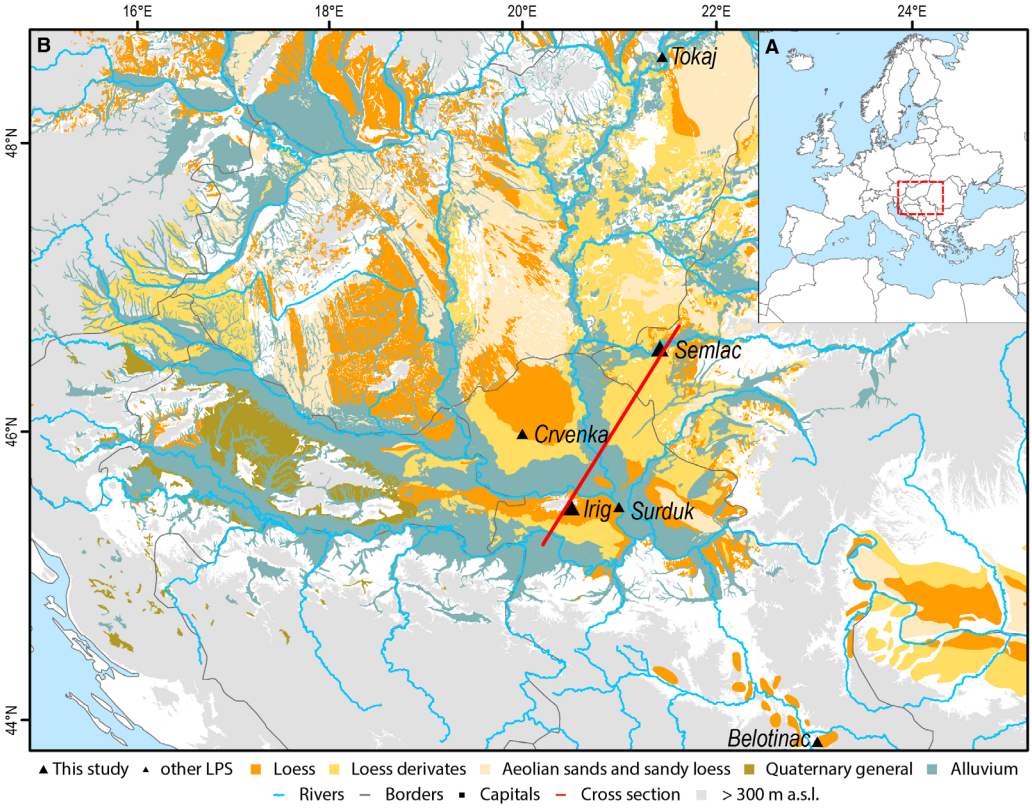
16°E
18°E
20°E
22°E
24°E
48°N
46°N
44°N
B
A
Tokaj
Semlac
Crvenka
Irig
Surduk
Belotinac
▲This study ▲ other LPS Loess Loess derivates Aeolian sands and sandy loess Quaternary general Alluvium
Rivers Borders Capitals Cross section > 300 m a.s.l.

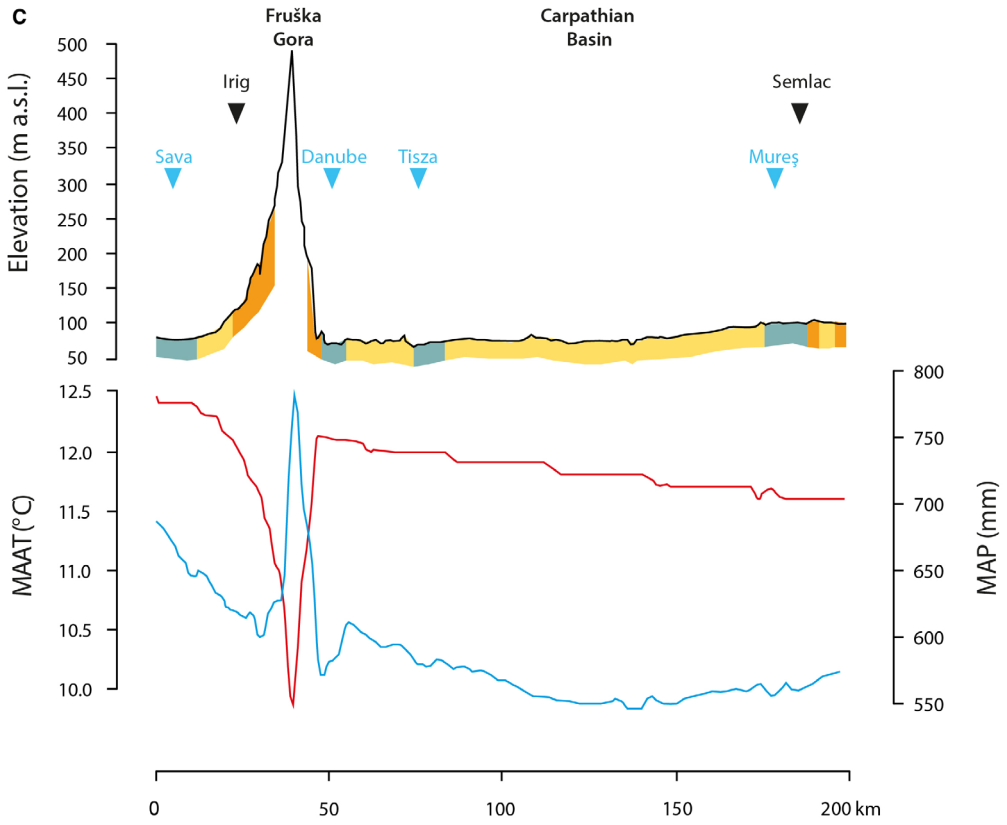
C
Fruška Gora
Carpathian Basin
Irig
Semlac
Sava
Danube
Tisza
Mureş
Elevation (m a.s.l.)
500
450
400
350
300
250
200
150
100
50
MAAT (°C)
12.5
12.0
11.5
11.0
10.5
10.0
MAP (mm)
800
750
700
650
600
550
0
50
100
150
200 km

Fig. 1. A. Location of the study area within Europe. B. Distribution of aeolian sediments in the study area (modified according to Haase *et al.* (2007) and Lehmkuhl *et al.* (2018)). Shown are both of the investigated LPS, Irig and Semlac, as well as other discussed LPS: Tokaj (Schatz *et al.* 2011), Crvenka (Zech *et al.* 2013; Marković *et al.* 2018), Surduk (Hatté *et al.* 2013) and Belotinac (Obreht *et al.* 2014). Elevations <300 m a.s.l. are shown as the upper topographic boundary for loess distribution and archaeological open-air findings in the Carpathian Basin (Hauck *et al.* 2017). C. Cross-sections of the topography and the outcropping Quaternary sediments (top) and the MAAT and MAP along a SW–NE transect (bottom). Climate gradients are derived from data by Karger *et al.* (2017). The location of the cross-section is indicated in panel B.

fication method (WC). The methods were used and compared with respect to their ability for complete decalcification.

A sample set from Irig ($n = 119$) was decalcified using pre-weighed silver capsules using the FM according to Harris *et al.* (2001). The Ag capsules containing ~50 mg of sample and a few drops of deionized water were placed in a desiccator together with a glass container filled with 36% HCl. The desiccator was placed under vacuum and the samples were left to react for 6 h. Finally, the samples were allowed to dry over a hot plate at ~50 °C; the capsules were crimped and the $\delta^{13}C$ analyses were carried out with a Carlo Erba NC 2500 elemental analyser coupled to a Delta^{plus} continuous flow isotope ratio mass spectrometer via a Conflow II interface (Thermo Finnigan MAT). The measurements were conducted at the Laboratory for Soil Science and Soil Geography at Bayreuth University (Germany).

All other WC preparation and geochemical measurements ($\delta^{13}C_{org}$, $\delta^{15}N_{bulk}$, TOC, TN) were performed in the laboratory of the Institute of Bio- and Geoscience, Forschungszentrum Jülich GmbH (Germany). Initially, 7 g of each sample was ground for 60 s at 80 r/min in a Retsch ball mill for homogenization. For the measurement of bulk nitrogen isotopes and the total nitrogen content, no further pretreatment was necessary. For the measurement of $\delta^{13}C_{org}$ and the total organic carbon (TOC) content samples were decalcified by wet chemical treatment. About 150 mg of each sample was weighed in centrifuge tubes, treated with 25 mL of hydrochloric acid (HCl, 5%) and kept in a 50 °C water bath for 4 h (see section Discussion - Methodological and reproducibility

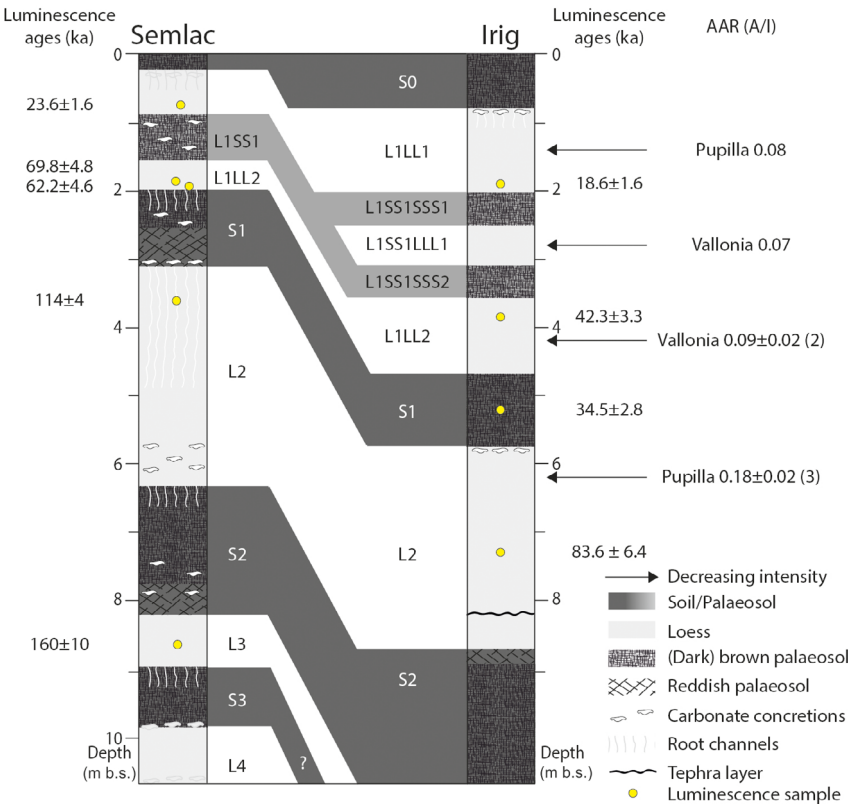

Fig. 2. Schematic stratigraphies of the Semlac and Irig LPS (simplified). Subunits are labelled according to the stratigraphical system of Marković *et al.* (2015). Published luminescence ages (Semlac: Zeeden *et al.* 2016; Irig: Marković *et al.* 2007) and total hydrolysate alloisoleucine/isoleucine (A/I) values for the gastropod genera *Pupilla* and *Vallonia* for Irig (Marković *et al.* 2007) are given. Note that the position of amino acid racemization and luminescence samples in Irig are given relative to the stratigraphical units, since the studied section is not the same as the section investigated by Marković *et al.* (2007).

Table 1. Summary of the results of the methodological tests (‰).

	Irig		Semlac	
	Fumigation method	Wet chemical acidification (4 h)	Wet chemical acidification (2 h)	Wet chemical acidification (4 h)
Mean	−20.2	−24.2	−24.6	−25.4
Maximum	−7.3	−22.8	−22.2	−23.2
Minimum	−25.4	−25.7	−25.6	−26.0
Range	18.1	2.9	3.4	2.8
SD	4.8	0.6	0.7	0.6

tests). Afterwards, samples were washed and centrifuged repeatedly with 45 mL of deionized water, in order to remove the remnants of the hydrochloric acid. Tubes were sealed with perforated tin foil, frozen at −20 °C and freeze-dried. Based on the tests described below method was used for decalcification in our study.

To ensure complete decalcification of our samples with this procedure, methodological tests concerning the efficiency with regard to the resistant carbonate siderite ($FeCO_3$) and the time of chemical treatment were conducted (Vuillemin *et al.* 2020). First, a technical grade, industrial sample of siderite with an initial carbon content of 8.7% was decalcified. About 200 mg of the sample was weighed in centrifuge tubes and treated with hydrochloric acid (25 mL, 5%) at 50 °C in the water bath. Treated samples were removed from the water bath in

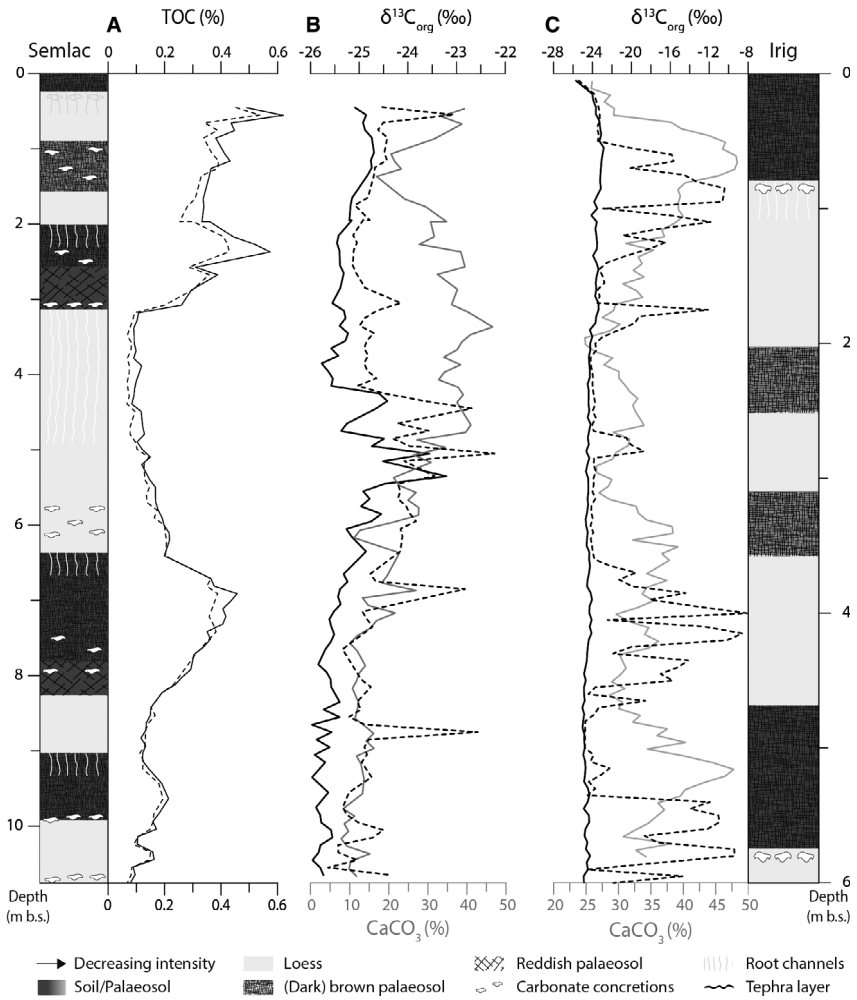

Fig. 3. The effects of different acidification treatments on TOC and $\delta^{13}C_{org}$ composition. A. TOC content from Semlac after 2 (dashed line) and 4 (solid line) h of wet chemical carbonate removal. B. $\delta^{13}C_{org}$ composition of Semlac after 2 (dashed line) and 4 (solid line) h of wet chemical carbonate removal. C. $\delta^{13}C_{org}$ composition of Irig after fumigation method (dashed line) and wet chemical carbonate removal (4 h, solid line). For B and C carbonate content (grey line) is given for comparison.

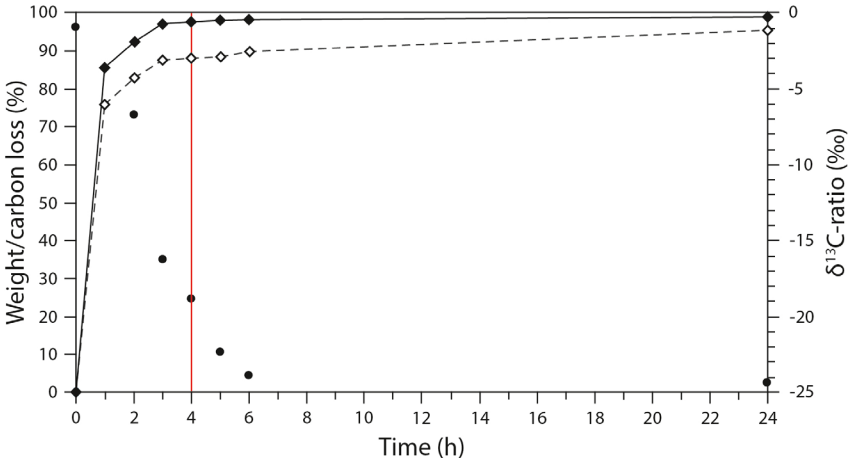

Fig. 4. Destruction of siderite by wet chemical acidification (20 mL HCl (5%), 50 °C) as a function of the treatment time (modified according to Vuillemin *et al.* (2020)). Given are total mass loss of siderite sample (open diamonds), loss of carbon (black diamonds) and the respective stable isotope composition (black circles). Note that total mass and carbon loss seem to be almost constant after 4 h, whereas the stable isotope composition declines further. The vertical red line marks the treatment duration finally chosen for this study (4 h).

duplicate every hour for a period of 6 h and again after 24 h. After washing and freeze-drying, mass loss, carbon content and $\delta^{13}C$ ratio of the residue were measured.

In order to transfer the findings from the siderite test to sediment samples, a set of samples from Semlac ($n = 95$) was treated with the WC decalcification as described above for 2 as well as for 4 h. Samples were chosen from the entire section. The TOC contents and the $\delta^{13}C$ ratio were measured to determine the impact of the longer treatment.

Additionally, a $\delta^{13}C_{org}$ reproducibility test was performed on conspicuous samples with low TOC contents from the Semlac profile ($n = 37$), which showed large scatter relative to the samples below or above. For these samples, subsamples were taken. For 12 of the samples, five subsamples were taken and two subsamples were analysed from another 25 of them. These samples were taken from layers with very low TOC content. All these 110 subsamples were treated with wet chemical acidification for 4 h. After washing and freeze-drying the TOC content as well as the $\delta^{13}C$ ratio of the residue were measured.

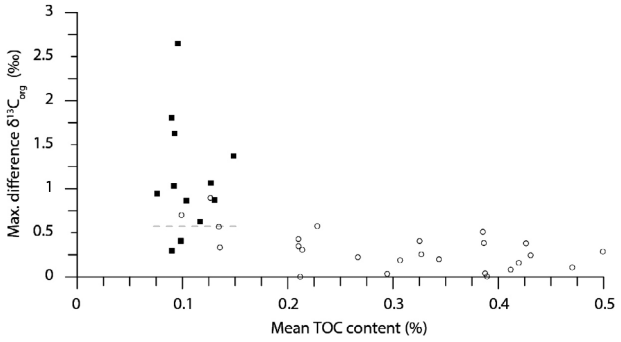

Fig. 5. Reproducibility of carbon isotope analysis given as maximal difference between replicates of single samples in relation to mean organic carbon content of the given samples. Black squares describe maximum difference for samples (TOC <0.15%) with five replicates, whereas open circles describe maximum difference for samples with two replicates. The grey dashed line shows the mean of mean replicate differences for samples with TOC <0.15%, which is 0.46‰, whereas the respective mean of the second sample set is 0.12‰.

Stable isotope and elemental measurements

Lyophilized samples were carefully homogenized with a spatula. An amount of sample to provide about 30 µg of nitrogen (typically 15–70 mg dry matter) was weighed into tin capsules for total nitrogen content (TN, in wt. %) and total nitrogen isotope ($\delta^{15}N_{bulk}$) determinations. Likewise, an amount of sample providing about 100 µg of organic carbon (typically 5–130 mg dry matter) was weighed in tin capsules for total organic carbon content (TOC, in wt. %) and organic carbon isotope ($\delta^{13}C_{org}$) analyses. The amounts of laboratory standards were adjusted accordingly to match the signal of the respective samples in the isotope-ratio mass spectrometer (IRMS). The packed samples were combusted at 1080 °C in an elemental analyser (Flash 200, Thermo Scientific) with automated sample supply linked to an IRMS (Delta V Plus, Thermo Scientific) for nitrogen and in an elemental analyser (EuroEA, Eurovector) with automated sample supply linked to an IRMS (Isoprime, Micromass) for carbon. Peak integration was used to determine TN and TOC contents and for calibration against elemental standards. All isotope results are reported in ‰ in the common δ notation according to the equation

$$\delta = \left(R_{sample}/R_{standard} - 1\right)x1000 \qquad (1)$$

where R is the isotope ratio ($^{13}C/^{12}C$, $^{15}N/^{14}N$) of the sample and standard, respectively. Calibrated laboratory

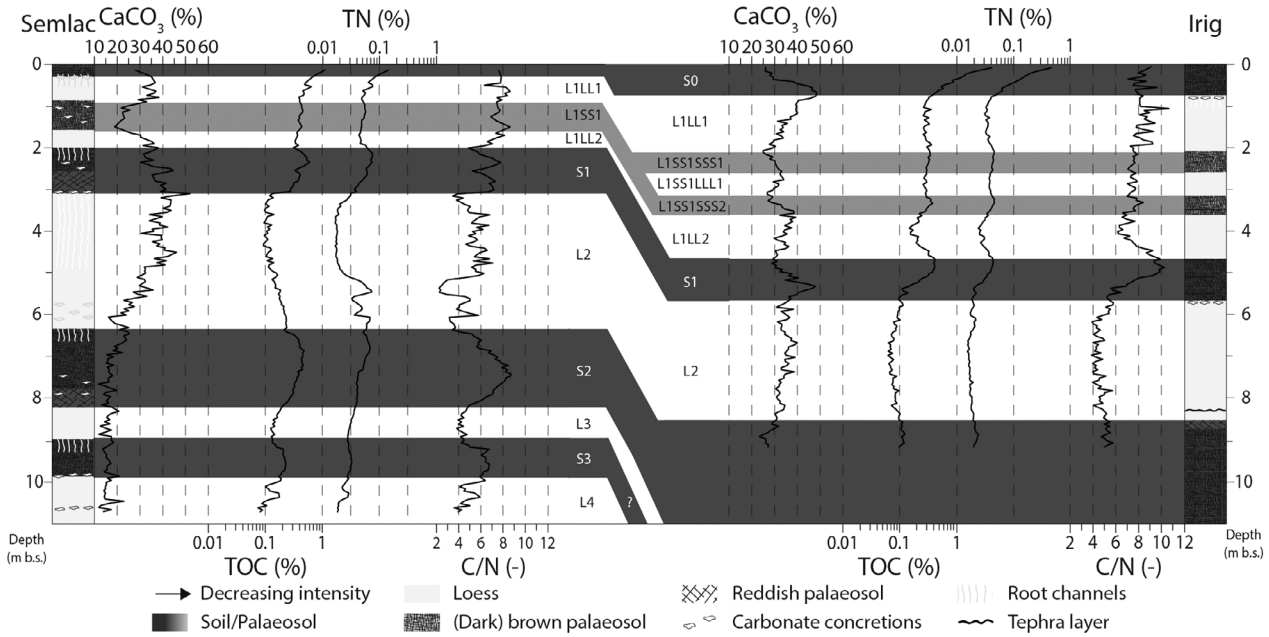

Fig. 6. Carbonate, TOC and TN contents as well as C/N ratio for the Semlac (left part) and Irig (right part) LPS. Stratigraphical correlation was done according to the stratigraphical system of Marković *et al.* (2015). Note the logarithmic scales for TOC and TN.

standards (Table S1) were used to ensure the quality of analyses and to scale-normalize the raw values to the isotopic reference scales VPDB for carbon and AIR for nitrogen. The general precision of replicate analyses is estimated to be better than 5% (rel.) for carbon and nitrogen content and <0.1‰ for $\delta^{15}N_{bulk}$ and $\delta^{13}C_{org}$, but considerably increases for samples with low TOC (see section Discussion - Methodological and reproducibility tests).

The loss of mass during decalcification is used as a proxy for and therefore equated with the carbonate content. Carbonate content analyses are based on the assumption that no other components such as iron oxides are removed during sample pretreatment. The TOC content is calculated using the carbon content of the decalcified sample (C_{org}) and the sample residue after decalcification ($HCl_{insoluble}$), using Equation 2:

$$TOC[\%] = C_{org}[\%]x\frac{HCl_{insoluble}[\%]}{100} \qquad (2)$$

Results

Methodological and reproducibility tests

The comparison of the FM to the WC shows remarkable differences between the two methods. The mean $\delta^{13}C_{org}$ value of the sample set decreases from −20.2‰ for the FM to −24.3‰ for the WC (Table 1). The $\delta^{13}C_{org}$ range declines by more than 15.0‰, namely from 18.1 to 2.9‰. In comparison to the WC (WC_{IR} 4 h), enriched values of up to −7.3‰ occur with the FM (Figs 3C, S1, S3). For both methods, the minimum isotope ratios show comparable values of −25.4 and −25.7‰ (Table 1).

The results of the siderite decalcification test are shown in Fig. 4. The (relative to calcium carbonate) more HCl-resistant siderite (Larson *et al.* 2008) was subsequently dissolved and after 4 to 6 h about 98% of the initial sample mass (impure siderite) was removed by the acid treatment. Accordingly, the $\delta^{13}C$-ratios decreased towards the signature of organic matter. Between 6 and 24 h, almost no further change can be observed. Considering that siderite concentrations in natural soil samples are generally low and not in the range of our test sample, these results show that the WC treatment effectively removes siderite and suggests a decalcification time between 2 to 4 h. This also avoids unnecessarily long treatment times that often bear the risk of secondary effects on the samples (Brodie *et al.* 2011).

To test the influence of the treatment time on actual loess and palaeosol samples, selected samples from Semlac were treated for 2 and for 4 h with the WC method. The results showed that a doubling of the treatment time overall leads to a small increase of the TOC content. The mean TOC value increased from 0.2 to 0.23% and the range increased from 0.47 to 0.53% (see Table 1). These differences are within the analytical uncertainty.

The influence of the treatment time on the $\delta^{13}C$ ratio is more notable as the mean value decreases from −24.6 to

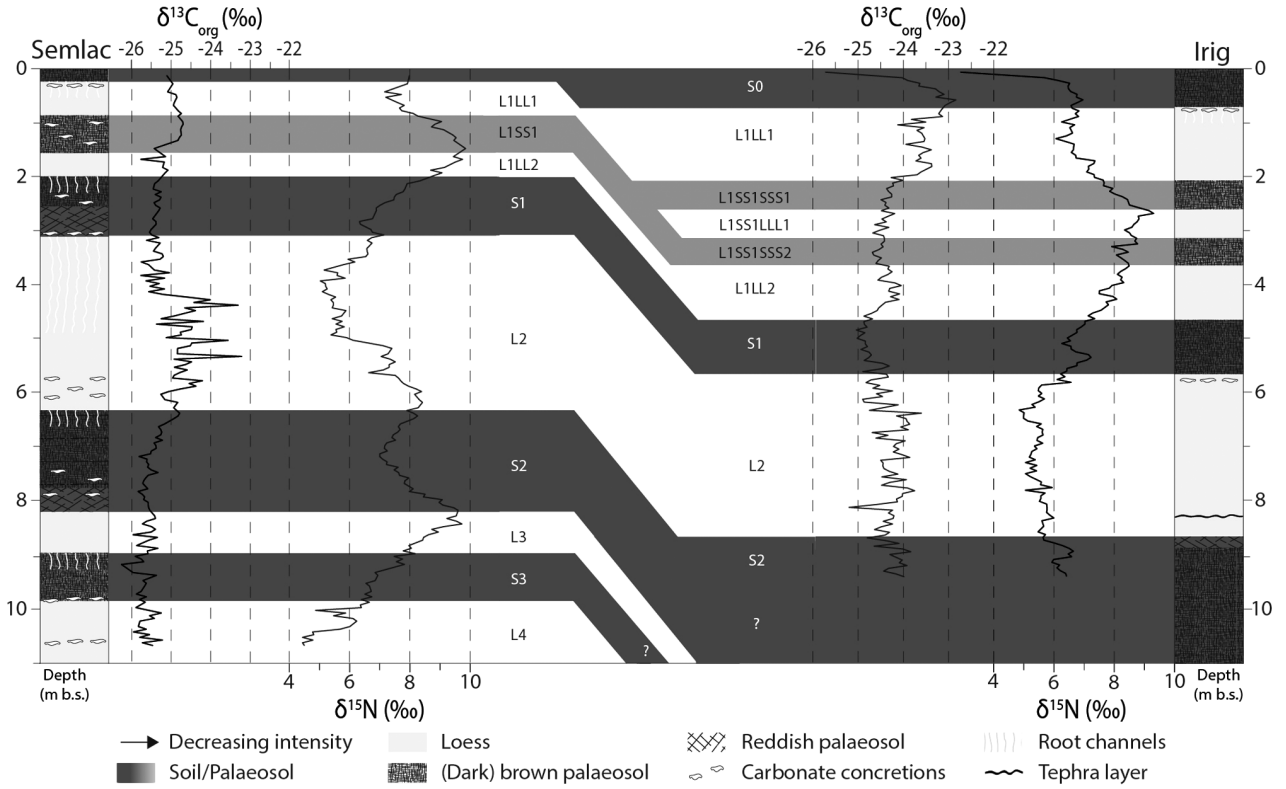

Fig. 7. Stable organic carbon ($\delta^{13}C_{org}$) and bulk nitrogen isotope ($\delta^{15}N$) compositions for Semlac (left part) and Irig (right part).

−25.4‰ and the range of variability narrowed down from 3.4 to 2.8‰ (Figs 3B, S2; Table 1). The longer treatment time might lead to additional carbon losses other than carbonates, which might explain the observed $\delta^{13}C_{org}$ changes. More likely, these results indicate that after 2 h of HCl treatment, traces of inorganic carbonates can still remain whereas after 4 h of HCl treatment decalcification of our samples is complete. Therefore, a treatment time of 4 h was eventually chosen for this study.

The $\delta^{13}C_{org}$ reproducibility test was conducted on selected samples from Semlac, with TOC contents ranging between 0.67 and 0.08%. Within the replicates, the TOC content showed variations with maximum differences ranging from 0.01 to 0.05%. The respective $\delta^{13}C_{org}$ values showed considerable variability between the replicates that is partly outside the analytical uncertainty. This is especially evident for samples with a mean TOC content of less than ~0.15% where the maximum spread within replicates of a single sample reaches up to 2.7‰ (Fig. 5, black squares). The respective mean of mean differences for replicates (n = 5) of this data set calculates to 0.46‰ (TOC <0.15%), whereas the mean of mean differences between replicates (n = 2) for the data set covering the whole TOC range (Fig. 5, open circles) shows an average of 0.12‰. This suggests that in LPS studies samples with low TOC contents (<0.15–0.2%) need higher replication to improve accuracy and precision of the respective $\delta^{13}C_{org}$ values.

Table 2. Overview of ranges of $\delta^{13}C$ ratios for different archives: loess organic matter (OM) from southeastern Europe, western Europe, China, Central Asia and the USA, from soil OM, loess bulk carbonates, loess earthworm granules and pedogenic carbonates. Note that the carbon isotope values for carbonates tend to higher values compared to OM.

	$\delta^{13}C$ ratio (‰)	References
Loess OM southeastern Europe	−27.0 to −21.0	This study, Zech *et al.* (2013), Obreht *et al.* (2014), Schatz *et al.* (2011), Hatté *et al.* (2013)
Loess OM western Europe	−25.4 to −16.9	Hatté *et al.* (2001), Pustovoytov & Terhorst (2004)
Loess OM China	−25.5 to −16	Weiguo *et al.* (2005), Youfeng *et al.* (2008), Gu *et al.* (2003)
Loess OM Central Asia	−26.1 to −19.5	Rao *et al.* (2013), Yang & Ding (2006)
Loess OM USA	−24 to −16	Muhs *et al.* (1999)
Soil OM	−28.0 to −13.4	Stevenson *et al.* (2005), Nordt *et al.* (1998), Midwood & Boutton (1998)
Loess bulk carbonates	−12.9 to 0	Frakes & Jianzhong (1994), Pustovoytov & Terhorst (2004), Rao *et al.* (2006)
Loess earthworm granules	−15.4 to −9.5	Prud'homme *et al.* (2018)
Pedogenic carbonates	−10.8 to +0.5	Stevenson *et al.* (2005), Ding & Yang (2000)

Geochemical analyses

Semlac. – The results for the carbonate content, TOC and TN as well as the C/N ratio are summarized in Fig. 6. The carbonate content in Semlac varies from 11.7% (7.65 m below surface (b.s.)) to more than 50% (directly underneath S1, ~3 m b.s.). The lower half of the section shows low carbonate contents. They exceed 20% only at the top of S2 and in several singular peaks in L3. In the upper half of the profile, a general enrichment of carbonate can be detected at the base or below palaeosols with the overall maximum right below S1. The top of the palaeosol is characterized by a slight decrease in carbonate, whereas the L1LL2 loess shows higher contents. The interstadial soil L1SS1 shows a decrease to around 20% compared to the overlying loess L1LL1.

The TOC follows the stratigraphy as relatively high values can be found in the recent topsoil (>1%) and the palaeosols. A generally increasing trend of TOC in the palaeosols compared is visible with decreasing depth (S3: >0.2%; S2: >0.4%; S1: >0.5%). The L3 loess shows a slight decline compared to the lowermost palaeosol. Within the loess layer, constant values of around 0.1 to 0.15% occur. The S2 palaeosol is characterized by an increase of TOC in the top of the soil, whereas the values at the base decrease to ~0.1%. The lower part of the L2 loess shows TOC contents of up to >0.2%, with a decreasing trend towards the top (0.1%). The S1 palaeosol shows a similar pattern as the S2, although the values are higher, and the soil is much thinner. The last glacial loess shows relatively high concentrations (0.25–0.4%) showing no clear distinction between the interstadial soil (L1SS1) and the loess packages (L1LL1 and L1LL2).

The total nitrogen (TN) content ranges from 0.01 to 0.15% and correlates strongly with the TOC content (r = 0.87). The lowermost part of the section shows a constant increase until the S2 palaeosol, which does not correspond to the TOC pattern. The S2 soil itself shows an increase, which corresponds to an increase in TOC in this layer. At a depth of around 5 m, the TN contents increase to up to 0.07%. Above, the L2 loess is characterized by constant values of 0.01%. Between the base of the S1 palaeosol to the top of the section TN is coherent with the TOC values.

The interglacial palaeosols S2 and S3 dominate the resulting C/N pattern of the lower half of the profile with striking maxima of >8 (S2) and >6 (S3).The C/N ratio shows a rather narrow range of 6 to >8 for the upper 3 m until the base of S1. Two local minima can be found at depths of 3–3.5 m (top L2) and at 5.2–5.7 m (base of L2).

The results of the measurements of carbon and nitrogen isotopes are summarized in Fig. 7. For the Semlac LPS, the $\delta^{13}C_{org}$ ratio varies between −26.3 and −23.2‰, with a mean value of −25.2‰. The carbon isotope signal shows no significant correlation to any other presented proxy (r_{TOC} = 0.0014; r_{TN} = 0.15; $r_{C/N}$ = 0.19; $r_{\delta 15N}$ = 0.03). The $\delta^{13}C_{org}$ ratio does not follow the stratigraphy, as the values in the lowermost part scatter from less than −26.0 to −24.8‰ without any clear trend. At the base of S2, the ratio reaches values of around −25.5‰. Within the soil, a slightly increasing trend towards the top is visible. Between 6 and 4 m, the carbon isotope ratios scatter strongly between −25.5‰ and the absolute maximum of −23.2‰. The uppermost part shows only a slightly increasing trend.

The $\delta^{15}N$ values show a stronger dependence on the stratigraphy. The values vary between 4.4‰ (10.55 m b.s.) and 9.9‰ (1.5 m b.s.), with an overall mean of 7.2‰. The basal part is characterized by a steady increase to values of >9‰. This is consistent throughout the top part of L4, the S3 palaeosol, as well as the L3 loess. The peak of this increase is at the base of S2, whereas the palaeosol itself is characterized by a minimum. The values increase again towards the top of the soil, forming a broad peak in the lower part of L2. The upper part of this loess layer is again characterized by constant, rather low values. At the base of S1, a small peak is visible, which is followed by a slight decrease. The values increase towards the top, reaching their absolute maximum in the L1SS1 palaeosol. Above, the ratios decrease again. $\delta^{15}N$ correlates weakly to moderately with TOC and TN (r_{TOC} = 0.44; r_{TN} = 0.53). The correlation to the C/N ratio is not significant for the whole sequence. Within the layers L2 and S2, however, the $\delta^{15}N$ ratio is strongly negatively correlated to the C/N ratio (r_{L2} = −0.67; r_{S2} = −0.7).

Irig. – The carbonate content in the Irig LPS varies from 23.1% in the S2 palaeosol to 56.6% below S1. In general, there is a trend of carbonate depletion visible within and an enrichment below the soils. Especially the thick loess packages show a decreasing trend with increasing depth. The thinner loess L1SS1LLL1, between the interstadial soils L1SS1SSS1 and L1SS1SSS2, shows a slightly increasing carbonate content with depth.

The base of the profile is characterized by constantly low TOC contents of ~0.1% throughout the upper part of S2 as well as the L2 loess. The interglacial S1 soil shows an increase to around 0.4%. The palaeosols L1SS1SSS1 and L1SS1SSS2 show only slight increases, whereas the last glacial loess layers show depleted values of around 0.3%. The highest TOC contents occur in the recent soil, exceeding values of 1.5%.

The total nitrogen content varies from 0.02% below S1 to 0.47% in the recent topsoil. In the lower part, below the S1 soil, the TN values are constantly low. In the L1LL1 as well as the L1LL2, the values are 0.3%, whereas in the layers between 1.75 and 3.25 m as well as the S1, the concentrations are around 0.4%. TN and TOC correlate very strongly (r = 0.99).

The resulting C/N ratio shows a scatter around a value of 8 with a maximum of more than 10 until a depth of 1.75 m. The lower part of the profile to its base is characterized by a slightly increasing tendency with depth, ranging between 4 and 6 (Fig. 6). The S1 soil is

characterized by a distinguished peak in C/N, followed by a rapid decline. The overlying loess shows a decrease of the ratio, whereas the L1SS1LLL2 soil shows a distinct increase. Between 4 and 1.75 m, a slight increase is visible. From the maximum at the depth of 1.75 m, the values are scattered to the top of the profile.

The lowest $\delta^{13}C$ ratios for Irig (−25.7‰) are located at the top of the profile within the S0. At the base of the recent topsoil, the maximum of −22.8‰ can be found (0.55 m) in the S0–L1LL1 transition. The variations within certain layers are larger in the lower half of the profile, with the strongest scatter between 5.5 and 6.5 m. The S2 palaeosol is characterized by a small increase in the isotopic ratio compared to the overlying loess. The transition towards the L2 is characterized by an increasing trend in isotopic composition, reaching values of >−24.0‰ at a depth of ~6 m. Within the S1 soil, the isotopic ratios are depleted compared to the loess package below. A small peak of around −24.0‰ is located within the L1LL2 loess. The ratios between the L1SS1SSS2 and L1SS1SSS1 increase towards the top, whereas the L1LL1 loess shows ratios varying around −24.5‰. The topsoil is in its lower parts characterized by values of <−23‰. The uppermost samples show the lowest ratios with the absolute minimum of −25.7‰. There is no significant correlation between $\delta^{13}C_{org}$ derived from the WC decalcification for 4 h and any other parameters (r_{TOC} = 0.014; r_{TN} = 0.0072; $r_{C/N}$ = 0.05, $r_{\delta 15N}$ = 0.03).

The $\delta^{15}N$ ratio for the Irig LPS varies between 2.9‰ in the recent topsoil and 9.3‰ in the L1SS1LLL1 loess layer. The mean value of all samples is 6.6‰. The S2 palaeosol is characterized by a small peak in nitrogen isotope ratios (~7.0‰). Within the L2 loess, the values are rather constant with a slightly decreasing tendency towards the top. In the upper part of L2, the values decrease again to a local minimum of ~5.0‰. The basal part of the S1 palaeosol shows a peak, whereas the upper part of the soil is characterized by decreasing values. Within the last glacial loess, the values increase towards the top and reach their absolute maximum in the transition between the L1SS1LLL1 loess layer and the palaeosol above. In the L1LL1 loess, the values decrease again and reach their absolute minimum in the uppermost samples of the recent topsoil. There is no correlation between $\delta^{15}N$ and TOC (r = 0.05) or TN (r = −0.06), but a medium-strong relationship between $\delta^{15}N$ and the C/N ratio (r = 0.54), especially within the L2 loess (r = 0.66).

Discussion

Methodological and reproducibility tests

The tests, regarding both the method of decalcification and the pretreatment time, show the significant influence of the decalcification method on the $\delta^{13}C_{org}$ signal. All $\delta^{13}C$ ratios, with one exception, were lowered when using the WC treatment instead of the FM and by the longer treatment during WC, (Figs 3, S1, S2). Inorganic carbonates in general have carbon isotope signatures between −15.0 and +0.5‰, whereas terrestrial organic matter has $\delta^{13}C$ values mainly between −28.0 and −25.0‰ (Table 2).

Thus, we conclude that the systematic shift towards lower organic carbon stable isotope values within our methodological tests are due to the incomplete removal of carbonates from the samples, especially with respect to the FM (Figs 3, S2, S3). The biasing effect of incomplete carbonate removal is clearly demonstrated by a comparison of $\delta^{13}C_{org}$ and C/N ratios of our test samples after FM and WC pretreatment (Fig. S3). A doubling of the treatment time of the WC caused a comparably minor further depletion of the $\delta^{13}C_{org}$ values with a small increase in TOC. This could point to residual carbonates in the samples. Overall, our tests show that the organic compounds of the sample were not destroyed or altered beyond the inevitable loss of organic matter inherent to any decalcification or drying pretreatment. Any method of decalcification removes carbon, either by volatilization of light organic compounds or by solution of easily soluble compounds. Since the TOC contents were not altered by a longer decalcification (Fig. 3A), we conclude that 4 h is a sufficient decalcification time for loess and palaeosol samples. These findings imply that the method of decalcification applied in stable isotope studies on LPS needs careful quality assessment to ensure complete removal of carbonates while preserving all organic matter within the samples. This is also crucial to avoid erroneous interpretation of e.g. C_4 plant organic matter contributions from spuriously enriched $\delta^{13}C_{org}$ values, or missing short episodes of C_4 vegetation.

Hatté *et al.* (1999) state that the $\delta^{13}C$ signal of soils and palaeosols can be altered due to ascending and especially descending translocation processes due to soil formation. These processes are also influenced by sedimentation rates. The higher the temporal resolution of the LPS, the higher is e.g. the distance from the respective layer to the associated topsoil. Our results show that even the underlying loess layers can be influenced by such leaching processes. Our reproducibility test further shows that especially layers with generic low TOC contents are prone to inaccurate or imprecise determination of organic carbon stable isotope values. Xie *et al.* (2004) and Liu *et al.* (2007) pointed out that rapid variations of the $\delta^{13}C$ signal could be due to the deposition of allochthonic dust with an inherent isotopic signal that can overprint the $\delta^{13}C$ ratio of the loess organic matter, even though the deposited material is very low in organic carbon. Thus, the observed peaks of the L2 layers at Semlac and Irig could either be due to allochthonic organic matter or due to the high scatter of the analytical results shown in the reproducibility test.

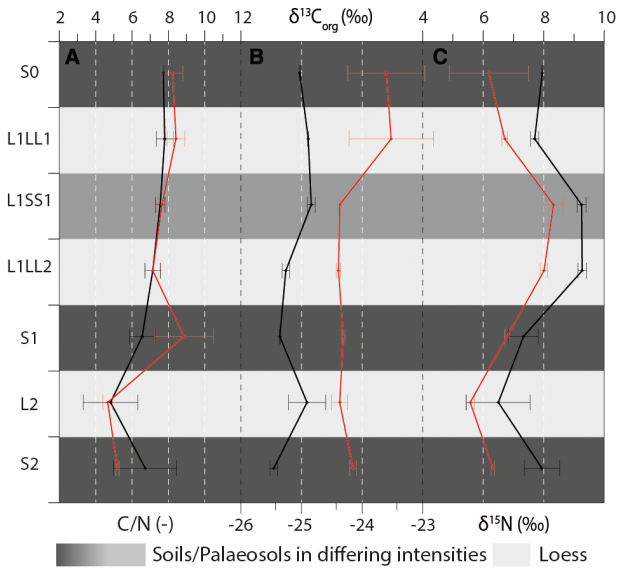

Fig. 8. Statistical comparison between (A) C/N ratio, (B) $\delta^{13}C_{org}$ ratio and (C) $\delta^{15}N$ ratio for Semlac (black) and Irig (red). Error bars indicate standard deviation.

Another possible source of these variations could be the influence of (grass) roots on the organic matter composition of the sediment. For Semlac, several such root channels were reported for the L2 loess. In Irig, however, no such observation was made. Due to the comparable stratigraphical position of the fluctuations in both sites and the absence of roots in Irig, this explanation seems rather unlikely. Since we observed a remarkably increased amplitude between replicates of the same sample with TOC contents <0.2% and not only high scatter between samples, the poor reproducibility seems to be caused by the natural sample inhomogeneity. Even though samples, especially from loess layers, appear to be homogeneous, slight inhomogeneities with regard to quantity and quality of the organic matter within one sample could lead to a large scatter of $\delta^{13}C_{org}$ values. Therefore, future studies should consider an increased replication for $\delta^{13}C_{org}$ measurements of samples with TOC contents <0.2%.

Palaeoenvironmental implications

The elemental carbon related records of Semlac and Irig partly show typical courses for LPS. The organic carbon content increases in the soils and palaeosols, whereas carbonate is enriched at the base of the soils due to secondary carbonate concretions as a result of e.g. leaching and re-precipitation during pedogenesis (e.g. Hatté *et al.* 2013). This clear trend however can only be detected within the upper half of Semlac, since the carbonate content and its fluctuations are much lower in the lower half, potentially due to deep-reaching leaching of carbonate. Even though a general decreasing trend in TOC is visible with depth in both profiles, all palaeosols are distinguishable from the underlying loess layers, potentially indicating higher biomass production (Schatz *et al.* 2011). The low contents of TOC and TN in the loess layers can also be attributed to dilution effects, where the organic matter is incorporated in the aeolian sediment. Due to high accumulation rates, the concentration of TOC is low, even though biomass production during loess deposition can sometimes be higher than expected from TOC contents (Zech *et al.* 2013). The C/N ratio, which is used as a proxy for the bacterial decomposition of organic matter (Vidic & Montañez 2004; Zech *et al.* 2007), shows that the decomposition in the interglacial soils in Semlac is rather low, as the high C/N ratios indicate no major loss of carbon or accumulation of nitrogen. For Irig, the S1 palaeosol shows similarly high values, whereas the S2 palaeosol is characterized by lower ratios. From the latter palaeosol, however, only the uppermost part was sampled. The depleted C/N ratio of the interstadial soils can be interpreted as the results of higher nitrogen accumulation during the microbial decomposition of the organic matter.

All the $\delta^{13}C_{org}$ ratios indicate a dominance of C_3 vegetation in the study area. The values are on the upper boundary of typical (modern) C_3 plants (O'Leary 1988). However, this comparison has to take into account the increase in atmospheric CO_2 concentrations in the industrial area that will have impacted the modern C_3 reference values. The pioneering work by O'Leary (1981, 1988) and Farquhar *et al.* (1989) were conducted at a time when the anthropogenically elevated atmospheric CO_2 concentration already influenced the vegetation (Ehlers *et al.* 2015). Compared to Late Pleistocene conditions, the recent CO_2 concentrations are elevated. The higher $\delta^{13}C$ ratios can be explained by the differences in the atmospheric conditions since lower CO_2 concentrations hamper fractionation of carbon isotopes and lead to elevated isotopic ratios (Jiang *et al.* 2019). However, the increased $\delta^{13}C$ ratios could also be a result of postdepositional degradation of biomass (Hatté *et al.* 1998, 1999; Hatté & Guiot 2005; Obreht *et al.* 2014). No major shifts towards a C_4 dominance can be detected.

Since the isotopic composition of the atmospheric CO_2 did not change significantly between glacials and interglacials (Leuenberger *et al.* 1992; Marino *et al.* 1992; Schneider *et al.* 2013), the concentration of CO_2, which shows a characteristic saw tooth pattern between glacials and interglacials (Petit *et al.* 1999), is more likely to affect the carbon isotope ratio in plants (Obreht *et al.* 2014). Feng & Epstein (1995) investigated empirically the effect of varying CO_2 concentrations on the isotope compositions of trees from California and Egypt. They concluded that an increase of 1 ppm in the atmospheric carbon dioxide content could lead to a decrease of the $\delta^{13}C$ of the trees of about 0.02‰ (Feng & Epstein 1995).

Since CO_2 concentrations vary by around 100 ppm between glacials and interglacials (Jouzel *et al.* 1993; Petit *et al.* 1999; Kawamura *et al.* 2007), the respective carbon isotope composition of biomass could be altered by up to 2‰. Especially for Irig, CO_2 and $\delta^{13}C$ behave inversely for the last two glacial cycles, indicating that atmospheric CO_2 was not the driving force of $\delta^{13}C$ distribution. Below S2 in Semlac, the isotopic ratio declines in a general trend with no visible relation to CO_2.

Studies on recent plant material along precipitation gradients in the USA (Stevenson *et al.* 2005) and China (Liu *et al.* 2005) indicate that the influence of the amount of annual rainfall on carbon isotopes declines when the values exceed 500 mm per year. Various studies regarding the reconstruction of palaeoprecipitation showed that a decrease of more than 200 mm compared to modern data is possible in glacial and interstadial times (Hatté & Guiot 2005; Kühn *et al.* 2013; Schatz *et al.* 2015). The effect of the palaeoprecipitation pattern can therefore not be neglected during the drier periods of the Pleistocene, since the low precipitation influences the isotopic ratio strongly.

Statistical tests of the mean values ($\delta^{13}C_{org}$, $\delta^{15}N$ and C/N ratio) for each lithological unit (Table S2), namely *F*-tests (Tables S3–S5) and Student's *t*-tests (Tables S6–S8) conducted on both sites show that there are significant differences between the two sites. A comparison of the recent climatic settings of both sections reveals that the section of Irig is nowadays in a more humid environment than Semlac, with a mean annual precipitation of around 690 mm compared to 590 mm in Semlac. Projecting the recent precipitation patterns to the carbon isotope ratios, the $\delta^{13}C_{org}$ ratio should be depleted in Irig compared to Semlac, since the enhanced moisture decreases the water stress. The stomata of the plants can be opened wider, and therefore a stronger fractionation against ^{13}C is possible, which leads to lower $\delta^{13}C_{org}$ values (O'Leary 1981; Farquhar *et al.* 1989). The results, however, reveal that the mean values for all layers in Irig are higher compared to Semlac, indicating drier conditions (Fig. 8). This is supported by $\delta^{13}C$ values from Crvenka (Zech *et al.* 2013) and Surduk sections (Hatté *et al.* 2013), which show similar values to the Irig section and suggest that the southern part of the Carpathian Basin was dryer than the rest of the basin. C_3 grasses, which are the most probable dust trap in the Carpathian Basin (Zech *et al.* 2013), tend to have higher $\delta^{13}C_{org}$ values under drier conditions (Wooller *et al.* 2007). The local palaeoclimate south of the Fruška Gora was drier compared to other parts of the Carpathian Basin (Marković *et al.* 2006, 2007, 2008; Vandenberghe *et al.* 2014), whereas the Petrovaradin LPS north of the mountain range shows evidence for more humid conditions during the last glacial cycle (Marković *et al.* 2005). Increasing wind exposure may be a crucial factor as well, since it has a negative correlation with the water availability (Zech *et al.* 2007), indicating that the local southeastern winds may play an important role in this region (Gavrilov *et al.* 2018). Other effects on the water availability, such as permafrost dynamics (Vinnepand *et al.* 2020), can be ruled out, based on the lack of periglacial features in the loess deposits of the southern Carpathian Basin.

The crossover temperature, i.e. the temperature of the growing season at which C_4 vegetation dominates, would be depleted during times with low atmospheric CO_2 concentrations. Nowadays, the crossover temperature is about 22 °C (Ehleringer *et al.* 1997; Collatz *et al.* 1998). Considering a crossover temperature of 18 °C for preindustrial times with an atmospheric CO_2 concentration of 270 ppm, the temperature can be interpolated for glacial (180 ppm) and interglacial (220–240 ppm) periods to 10 and 12–13 °C, respectively (Obreht *et al.* 2014). The dominance of C_3 vegetation at Irig indicates that the temperatures for the growing season, which in glacial times equals the summer months, was probably below 15 °C during the major part of the last glacial, and likely in a range from 10–13 °C during the last glacial maximum. These palaeotemperatures are on the one hand in accordance with temperatures for interstadial periods from Nussloch in Germany, reconstructed from $\delta^{18}O$ isotopic ratios of earthworm granules (Prud'homme *et al.* 2016). On the other hand, these data indicate that the Carpathian Basin was notably warmer during the stadials and especially the last glacial maximum, when compared to western Europe. The dominance of C_3 vegetation, however, contradicts Marković *et al.* (2007), who assumed summer temperatures of more than 15 °C in Irig, based on malacological data. Especially the dominance of *Chondrula tridens* and *Helicopsis striata* faunae in Irig indicates warm conditions since these species are indicative of interstadials in central Europe (Ložek 2001). Since the site lacks transitional and cold-resistant species that can be found in the malacological faunae of nearby loess sections, it was argued that the comparably dry southern slope of the Fruška Gora acted as an ecological refugium for warmth-loving species (Marković *et al.* 2007, 2008). The contradictive crossover temperature derived from the stable carbon isotope records indicates that the dominance of thermophilic molluscs was not only controlled by temperature, but also by aridity.

Not only the carbon isotope composition with its more negative values leads to the conclusion of drier palaeoclimatic conditions in Irig, but also the grain size and magnetic data as well as the palaeopedological field observations from Semlac support this thesis (Zeeden *et al.* 2016). Striking evidence for this is e.g. the remarkable soil formation during MIS 3 in Semlac (Schulte & Lehmkuhl 2018). Within the southeastern Carpathian Basin, no comparable thick or intense palaeosol is reported. In Irig, e.g. the MIS 3 is imprinted as a soil complex, intercalated with a distinct loess layer, indicat-

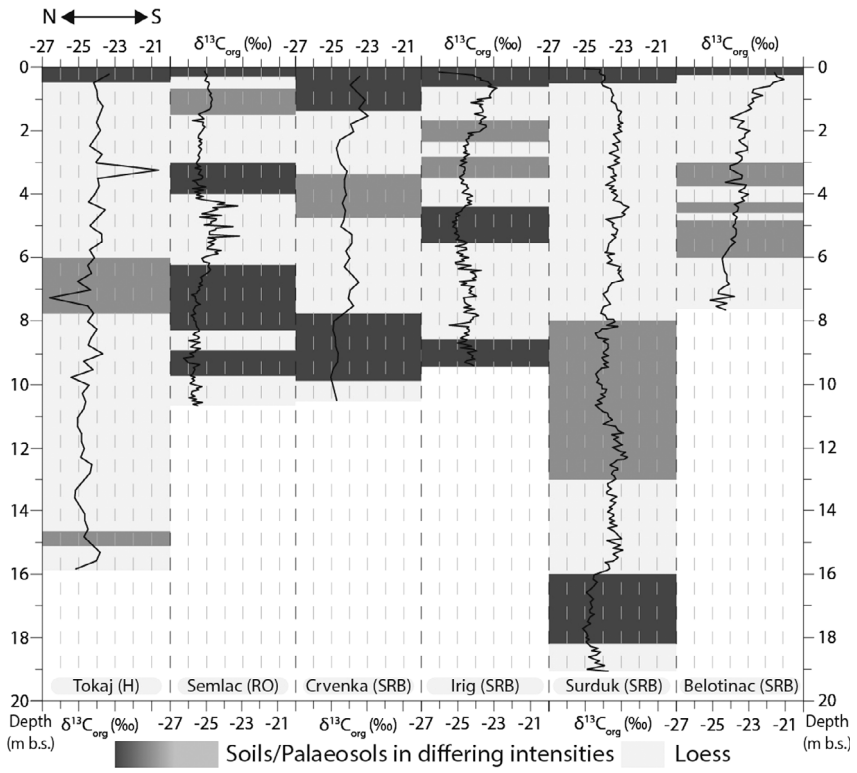

Fig. 9. Comparison of the organic stable carbon isotope records from the Carpathian Basin: Tokaj (Schatz *et al.* 2011), Semlac (this study), Crvenka (Zech *et al.* 2013), Irig (this study), Surduk (Hatté *et al.* 2013) and Belotinac (Obreht *et al.* 2014), sorted from north to south.

ing drier conditions during MIS 3. The location of Semlac nearby the western foothills of the Carpathians in combination with predominating winds from northwest (Sebe *et al.* 2011; Gavrilov *et al.* 2018) and southeast (Obreht *et al.* 2015; Gavrilov *et al.* 2018), are most likely to explain the differences in (palaeo-)moisture regimes of both sites. The sediments in Semlac are generally influenced by long-range transport, with fine, homogeneous loess layers (Schulte *et al.* 2014; Zeeden *et al.* 2016), whereas the source areas of LPS of the southern Carpathian Basin are usually the nearby fluvial deposits within the basin (Obreht *et al.* 2019). This variation could be a reason for the large scatter between 4 and 6 m in Semlac, since allochthonous organic matter can superimpose the *in-situ* signal, even if the TOC content is low (Xie *et al.* 2004; Liu *et al.* 2007). No systematic change, either in climate or vegetation, could be linked reliably to these fluctuations. All these peaks, however, are in the range detected by the reproducibility test. Even though the reproducibility test was not conducted for samples from Irig, the same issues should be considered here. The low TOC contents (0.1%) indicate that the same analytical issues may affect the L2 layer as the corresponding layer in Semlac. Additionally, the $\delta^{13}C_{org}$ ratio in Irig could also be influenced by allochthonous organic matter within the deposited dust (Xie *et al.* 2004; Liu *et al.* 2007).

Although the dominant pathway of photosynthesis of the palaeovegetation appears to be constant throughout glacial cycles at both sections, the qualities of the respective ecosystems seem to differ quite strongly. The $\delta^{15}N$ record is dependent on these qualities, especially the openness of the nitrogen cycle. Open N-cycles occur in ecosystems with significant inputs or losses of nitrogen. This leads to higher $\delta^{15}N$ values in the soil organic matter (Zech *et al.* 2011). The source of nitrogen also influences the isotopic composition, since e.g. nitrogen that is biologically fixed as N_2 has a $\delta^{15}N$ ratio of $0\pm2‰$, whereas other N sources are highly variable (Amundson *et al.* 2003). Additionally, the nitrogen isotope ratio seems to be partly controlled by the climate. For sites with a MAAT >0.5 °C, increasing temperatures produce decreasing stable nitrogen values. The same relationship is observed for annual precipitation (Amundson *et al.* 2003; Craine *et al.* 2009). The nitrogen isotope ratios for Irig are generally lower than for Semlac (Fig. 8), leading to the conclusion that Semlac has a general tendency to more open N-cycles or that water availability is the key factor in isotopic differences between the two sites, which is also supported by the carbon isotopes.

It is striking that the nitrogen isotope signal is strongly connected to general climatic trends, with generally depleted ratios in the loess layers and elevated values in the palaeosols, especially at the

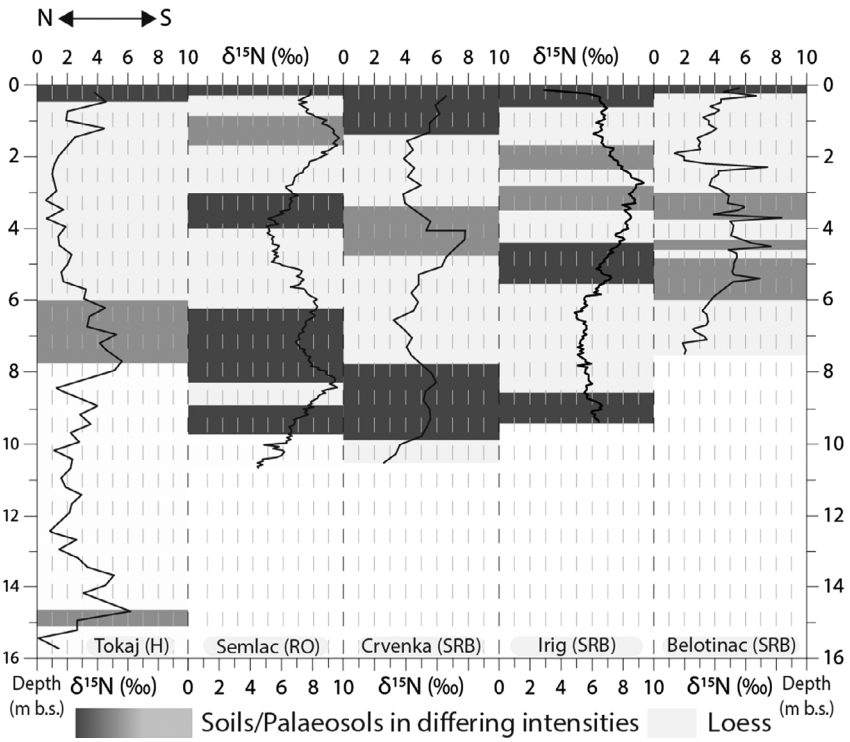

Fig. 10. Comparison of the nitrogen isotope records from the Carpathian Basin: Tokaj (Schatz *et al.* 2011), Semlac (this study), Crvenka (Zech *et al.* 2013), Irig (this study) and Belotinac (Obreht *et al.* 2014), sorted from north to south.

bases. This is in agreement with findings from recent soils, where the $\delta^{15}N$ ratio increases with depth (Amundson *et al.* 2003). These variations show the interplay between soil (forming) processes and the nitrogen isotopic composition. High mineralization rates in soils as well as high input rates of nitrogen lead to higher N release. For Semlac, the lowest values are measured in the L4, increasing gradually to S3. Untypically, the L3 loess package also shows a steady increase, but this could be due to leaching effects of organic matter in the form of particles, colloids or dissolved organic matter (OM) from the thick interglacial S2 palaeosol above, which shows the highest values at the transition to L3. The elevated values at the base of L2 partially support the hypothesis of the impact of allochthonous organic matter on palaeoecological proxies such as the isotope ratios since they partially coincide with the high scatter of $\delta^{13}C_{org}$ in Semlac. In the upper part of L2, no clear connection between the two proxies is visible. This could be a result of different compositions of the allochthonous material. However, the missing clear differentiation between the sources of deflated dust hampers a clear link. In Irig, only a small increase is visible in the upper part of S2 and almost no variations can be seen in the L2 loess layer. This may be an indicator of a dilution of the signal, due to the higher accumulation rates compared to the input of organic material. The low TOC and TN values with almost no spread also support this dilution.

Interestingly, the trends of the nitrogen isotope values between Irig and Semlac is very similar for the last glacial cycle: the S1 palaeosol is characterized by a peak at the base, which extends to the lower part of the soil. After a local minimum, the ratio increases again and has its (absolute) maximum value within the MIS 3 pedocomplex. The high values corresponding to palaeosols indicate a higher productivity of the ecosystem. The higher demand for nitrogen lowers the discrimination against ^{15}N and increases the use of nitrate (enriched compared to ammonium) and, therefore, leads to an increase of the $\delta^{15}N$ ratio (Obreht *et al.* 2014). This is, compared to the loess packages, a result of more favourable temperature regimes, especially during the vegetation period. These climatic differences also lead to enhanced pedogenesis and therefore nitrogen losses e.g. in gaseous state. The differences between interglacial and interstadial palaeosols point to different palaeoclimatic dynamics. Alternatively, it has been reported that $\delta^{15}N$ values are also positively correlated with mean annual temperature and negatively with mean annual precipitation (Houlton *et al.* 2007; Zhou *et al.* 2014; Liu & Liu 2017). The $\delta^{15}N$ ratio shows a stronger enhancement in the MIS 3 interstadial compared to interglacial soils, suggesting that the increase in the mean annual temperature during periods of soil formation was not the main

driving force for $\delta^{15}N$ enhancements. However, the mean annual precipitation was likely remarkably lower during MIS 3 than during interglacial soil formation throughout most of the Carpathian Basin, leading to cooler but drier conditions. Since the soil types e.g. in Irig of the MIS 3 soil complex (L1SS1SSS1, L1SS1SSS2) and the S2 are all described as chernozem (like), it can be postulated that the precipitation variations influenced the nitrogen cycling of the vegetation, but not the soil formation process. This supports studies stating that the area was continuously dominated by steppe environments and grasslands (Zech *et al.* 2013; Marković *et al.* 2018).

Comparison to other archives

Most of the stable isotope studies from the Carpathian Basin indicate the same palaeovegetation pattern as our study, with a predominance of C_3-vegetation throughout the basin, especially for the last glacial cycle and the last 45 ka in particular (Fig. 9). Although excursions to C_4-vegetation cannot be ruled out completely (Hatté *et al.* 2013; Obreht *et al.* 2014), no major shifts could be detected by any of the studies. Only Hatté *et al.* (2013) showed excursions to C_4-vegetation in their data set from Surduk and related them to changes in atmospheric circulations during the Late Pleistocene. These differences can be mostly related to the higher resolution of the study, resulting from higher sedimentation rates in Surduk during the Last Glacial cycle (Antoine *et al.* 2009). The Carpathian Basin seems to have acted as a refuge for C_3-vegetation. Other regions, such as Central Asia, China or the United States show clearer indications for C_4-vegetation derived from stable carbon isotope ratios from loess organic matter, especially during glacial times (Table 2).

The $\delta^{15}N$ records of Semlac and Irig show comparable results to the other archives from the Carpathian Basin (Schatz *et al.* 2011), even though the temporal scales of the archives differ (Fig. 10). For example, the LPS of Crvenka (Zech *et al.* 2013; Marković *et al.* 2018) also shows enhanced values in the palaeosol, especially the L1SS1. In general, the nitrogen isotope ratios for Semlac and Irig are higher than for the other archives, which can be explained by higher accumulation rates compared to our study sites. All compared sequences show, only based on the stratigraphical succession, higher deposition rates of mineral dust compared to Irig and Semlac. Therefore, the relative input of organic matter and consequently nitrogen was reduced for these sections, which led to a lower isotopic ratio.

Conclusions

Our study shows that for carbon isotope analyses on loess-palaeosol sequences a detailed quality control of the applied methods is crucial, including a critical evaluation of the applied pretreatment methods. Our results preclude the fumigation method as an appropriate method for complete carbonate removal from loess and palaeosol samples, especially for samples with high contents of inorganic carbon. The completeness of decalcification should be tested for both loess and palaeosol layers, since the content, the mineralogy and other characteristics of carbonates can differ significantly between different sites. Moreover, we find that $\delta^{13}C_{org}$ values of aliquots samples with a generic low TOC can scatter by several per mil. This could be due to analytical artefacts but is more likely the result of the heterogeneity of geological samples. Irrespectively, the weak reproducibility recommends extended reproducibility tests to obtain reliable results for such samples. The influence of e.g. allochthonous dust and its overprinting of the *in-situ* organic carbon isotope ratio can also not be ruled out. To ensure the reliability of comparisons between archives and (supra-)regional palaeoecological overviews, methodological and reproducibility tests should be always reported. This leads to the conclusion that stable carbon isotope studies can also be applied to older sediments from the Carpathian Basin.

Our study confirms the dominance of C_3-vegetation in the Carpathian Basin during the Middle to Late Pleistocene. Although we cannot fully rule out the presence of C_4-vegetation completely by using proxy-data, e.g. due to dilution effects, no gradual, systematic or rapid shifts towards a vegetation using another dominant photosynthesis pathway are indicated by our data, neither in Irig nor in Semlac. Our results, however, show indications of a continuously drier palaeoclimate in Irig, compared to Semlac. These differences can be explained by hydroclimatic gradients in the Carpathian Basin during the Pleistocene. The southern part of the basin, and especially the southern slopes of the Fruška Gora on which Irig is situated, acted as a biogeographical refugium for thermophilic mollusc species, even though the July temperatures were not much higher than in the rest of the basin. This indicates that the abundance of thermophilic species is not only governed by the temperature, but also by aridity. Despite these differences, no major oscillations at either site were detected by the stable carbon isotope ratios, in contrast to other proxies, which reflect fluctuations between glacials/stadials and interglacials/interstadials. For the southern Carpathian Basin, it seems that the responses of the vegetation to climatic fluctuations were not sensitive enough to be detected by this method. The interpretation of past environmental conditions is always constrained by specific environmental and temporal scales, depending on the analytical methods used and the ecological processes on which the method is based. Other environmental proxies, e.g. the malacofaunal abundance, can only be reliably compared to stable carbon isotope records when these different environmental and temporal scales are considered. The nitrogen isotope ratios,

however, show a more differentiated pattern, where the reconstructed ecosystem qualities seem to reflect more the general palaeoclimatic dynamics. Especially the interstadials are well represented by this ratio and seem to reflect more humid phases compared to the stadials. The interpretation of this complex proxy, however, needs more systematic studies in loess deposits worldwide.

Acknowledgements. – The investigations were carried out in the framework of the CRC 806 'Our way to Europe', subproject B1 'The Eastern Trajectory': 'Last Glacial Palaeogeography and Archaeology of the Eastern Mediterranean and of the Balkan Peninsula', funded by the Deutsche Forschungsgemeinschaft (DFG, German Research Foundation) – Projektnummer 57444011 – SFB 806. We thank D. Haase for providing the shapefiles for Fig. 1. Jonas Viehweger helped by compiling Fig. 1. We thank Janina Bösken for her helpful comments, which improved the manuscript. Finally, we are grateful to the two anonymous reviewers and Prof. Jan A. Piotrowski as editor-in-chief for their helpful comments, which greatly improved the quality of the figures and the manuscript. Open access funding enabled and organized by Projekt DEAL.

Author contributions. – FL and AL designed the study. AL and HW developed the methodological framework of the study. IO, MZ and SBM carried out the fieldwork. AS, AL, HW and MZ conducted the elemental and isotopic measurements and methodological tests. SP and PS developed the structure of the manuscript. SP wrote the manuscript and drew the figures. All authors discussed and revised the manuscript.

Data availability statement. – The isotopic composition data for both loess-palaeosol sequences are available from the CRC806 database at https://doi.org/10.5880/sfb806.50.

References

Amundson, R., Austin, A. T., Schuur, E. A. G., Yoo, K., Matzek, V., Kendall, C., Uebersax, A., Brenner, D. & Baisden, W. T. 2003: Global patterns of the isotopic composition of soil and plant nitrogen. *Global Biogeochemical Cycles 17*, 1031, https://doi.org/10.1029/2002GB001903.

Andreeva, D., Zech, M., Glaser, B., Erbajeva, M., Chimitdorgieva, G., Ermakova, O. & Zech, W. 2013: Stable isotope ($\delta^{13}C$, $\delta^{15}N$, $\delta^{18}O$) record of soils in Buryatia, southern Siberia: implications for biogeochemical and paleoclimatic interpretations. *Quaternary International 290–291*, 82–94.

Antoine, P., Rousseau, D.-D., Fuchs, M., Hatté, C., Gauthier, C., Marković, S. B., Jovanović, M., Gaudenyi, T., Moine, O. & Rossignol, J. 2009: High-resolution record of the last climatic cycle in the southern Carpathian Basin (Surduk, Vojvodina, Serbia). *Quaternary International 198*, 19–36.

Aranibar, J. N., Otter, L., Macko, S. A., Feral, C. J. W., Epstein, H. E., Dowty, P. R., Eckhardt, F., Shugart, H. H. & Swap, R. J. 2004: Nitrogen cycling in the soil-plant system along a precipitation gradient in the Kalahari sands. *Global Change Biology 10*, 359–373.

Beck, J. W., Zhou, W., Li, C., Wu, Z., White, L., Xian, F., Kong, X. & An, Z. 2018: A 550,000-year record of East Asian Monsoon rainfall from ^{10}Be in loess. *Science 360*, 877–881.

Bergerat, F. 1989: From pull-apart to the rifting process: the formation of the Pannonian Basin. *Tectonophysics 157*, 271–280.

Bösken, J., Obreht, I., Zeeden, C., Klasen, N., Hambach, U., Sümegi, P. & Lehmkuhl, F. 2019: High-resolution paleoclimatic proxy data from the MIS3/2 transition recorded in northeastern Hungarian loess. *Quaternary International 502*, 95–107.

Bösken, J., Sümegi, P., Zeeden, C., Klasen, N., Gulyás, S. & Lehmkuhl, F. 2017: Investigating the last glacial Gravettian site "Ságvár Lyukas Hill" (Hungary) and its paleoenvironmental and geochronological context using a multi-proxy approach. *Palaeogeography, Palaeoclimatology, Palaeoecology 509*, 77–90.

Brodie, C. R., Leng, M. J., Casford, J. S. L., Kendrick, C. P., Lloyd, J. M., Yongqiang, Z. & Bird, M. I. 2011: Evidence for bias in C and N concentrations and $\delta^{13}C$ composition of terrestrial and aquatic organic materials due to pre-analysis acid preparation methods. *Chemical Geology 282*, 67–83.

Buggle, B., Glaser, B., Hambach, U., Gerasimenko, N. & Marković, S. B. 2011: An evaluation of geochemical weathering indices in loess–paleosol studies. *Quaternary International 240*, 12–21.

Buggle, B., Glaser, B., Zöller Hambach, U., Marković, S. B., Glaser, I. & Gerasimenko, N. 2008: Geochemical characterization and origin of Southeastern and Eastern European loesses (Serbia, Romania, Ukraine). *Quaternary Science Reviews 27*, 1058–1075.

Cerling, T. E. 1984: The stable isotopic composition of modern soil carbonate and its relationship to climate. *Earth and Planetary Science Letters 71*, 229–240.

Chu, W. 2018: The Danube corridor hypothesis and the Carpathian Basin: geological, environmental and archaeological approaches to characterizing Aurignacian dynamics. *Journal of World Prehistory 31*, 117–178.

climate-data.org. 2019: *Climate Arad*. https://de.climate-data.org/europa/rumaenien/arad/arad-163/#climate.

Collatz, G. J., Berry, J. A. & Clark, J. S. 1998: Effects of climate and atmospheric CO_2 partial pressure on the global distribution of C_4 grasses: present, past, and future. *Oecologia 114*, 441–454.

Craine, J. M., Elmore, A. J., Aidar, M. P. M., Bustamante, M., Dawson, T. E., Hobbie, E. A., Kahmen, A., Mack, M. C., McLauchlan, K. K., Michelsen, A., Nardoto, G. B., Pardo, L. H., Peñuelas, J., Reich, P. B., Schuur, E. A. G., Stock, W. D., Templer, P. H., Virginia, R. A., Welker, J. M. & Wright, I. J. 2009: Global patterns of foliar nitrogen isotopes and their relationships with climate, mycorrhizal fungi, foliar nutrient concentrations, and nitrogen availability. *New Phytologist 183*, 980–992.

Craine, J. M., Elmore, A. J., Wang, L., Augusto, L., Baisden, W. T., Brookshire, E. N. J., Cramer, M. D., Hasselquist, N. J., Hobbie, E. A., Kahmen, A., Koba, K., Kranabetter, J. M., Mack, M. C., Marin-Spiotta, E., Mayor, J. R., McLauchlan, K. K., Michelsen, A., Nardoto, G. B., Oliveira, R. S., Perakis, S. S., Peri, P. L., Quesada, C. A., Richter, A., Schipper, L. A., Stevenson, B. A., Turner, B. L., Viani, R. A. G., Wanek, W. & Zeller, B. 2015: Convergence of soil nitrogen isotopes across global climate gradients. *Scientific Reports 5*, 8280, https://doi.org/10.1038/srep08280.

Delwiche, C. C. & Steyn, P. L. 1970: Nitrogen isotope fractionation in soils and microbial reactions. *Environmental Science & Technology 4*, 929–935.

Ding, Z. L. & Yang, S. L. 2000: C_3/C_4 Vegetation evolution over the last 7.0 Myr in the Chinese Loess Plateau: evidence from pedogenic carbonate $\delta^{13}C$. *Palaeogeography, Palaeoclimatology, Palaeoecology 160*, 291–299.

Ding, Z. L., Ranov, V., Yang, S. L., Finaev, A., Han, J. M. & Wang, G. A. 2002: The loess record in southern Tajikistan and correlation with Chinese loess. *Earth and Planetary Science Letters 200*, 387–400.

Dolton, G. L. 2006: Pannonian Basin province, central Europe (Province 4808) — petroleum geology, total petroleum systems, and petroleum resource assessment. *U.S. Geological Survey, Bulletin 2204–B*, 1–47.

Ehleringer, J. R., Cerling, T. E. & Helliker, B. R. 1997: C_4 photosynthesis, atmospheric CO_2, and climate. *Oecologia 112*, 285–299.

Ehlers, I., Augusti, A., Betson, T. R., Nilsson, M. B., Marshall, J. D. & Schleucher, J. 2015: Detecting long-term metabolic shifts using isotopomers: CO_2-driven suppression of photorespiration in C_3 plants over the 20th century. *Proceedings of the National Academy of Sciences 112*, 15585–15590.

Evans, R. D. 2001: Physiological mechanisms influencing plant nitrogen isotope composition. *Trends in Plant Science 6*, 121–126.

Farquhar, G. D., Ehleringer, J. R. & Hubick, K. T. 1989: Carbon isotope discrimination and photosynthesis. *Annual Review of Plant Physiology and Plant Molecular Biology 40*, 503–537.

Feng, X. & Epstein, S. 1995: Carbon isotopes of trees from arid environments and implications for reconstructing atmospheric CO_2 concentration. *Geochimica et Cosmochimica Acta 59*, 2599–2608.

Frakes, L. A. & Jianzhong, S. 1994: A carbon isotope record of the upper Chinese loess sequence: estimates of plant types during stadials and interstadials. *Palaeogeography, Palaeoclimatology, Palaeoecology 108*, 183–189.

Gábris, G. 1994: Pleistocene evolution of the Danube in the Carpathian Basin. *Terra Nova 6*, 495–501.

Gallet, S., Jahn, B. & Torii, M. 1996: Geochemical characterization of the Luochuan loess-paleosol sequence, China, and paleoclimatic implications. *Chemical Geology 133*, 67–88.

Gauthier, C. & Hatté, C. 2008: Effects of handling, storage, and chemical treatments on $\delta^{13}C$ values of terrestrial fossil organic matter. *Geochemistry, Geophysics, Geosystems 9*, Q08011, https://doi.org/10.1029/2008GC001967.

Gavrilov, M. B., Marković, S. B., Schaetzl, R. J., Tošić, I., Zeeden, C., Obreht, I., Sipos, G., Ruman, A., Putniković, S., Edmunds, K., Perić, Z., Hambach, U. & Lehmkuhl, F. 2018: Prevailing surface winds in Northern Serbia in the recent and past time periods; modern- and past dust deposition. *Aeolian Research 31*, 117–129.

Gu, Z., Liu, Q., Xu, B., Han, J., Yang, S., Ding, Z. & Liu, T. 2003: Climate as the dominant control on C_3 and C_4 plant abundance in the Loess Plateau: organic carbon isotope evidence from the lastglacial-interglacial loess-soil sequences. *Chinese Science Bulletin 48*, 1271–1276.

Haase, D., Fink, J., Haase, G., Ruske, R., Pécsi, M., Richter, H., Altermann, M. & Jäger, K.-D. 2007: Loess in Europe—its spatial distribution based on a European loess map, scale 1:2,500,000. *Quaternary Science Reviews 26*, 1301–1312.

Han, J., Keppens, E., Tungsheng, L., Paepe, R. & Wenying, J. 1997: Stable isotope composition of the carbonate concretion in loess and climate change. *Quaternary International 37*, 37–43.

Harris, D., Horwáth, W. R. & van Kessel, C. 2001: Acid fumigation of soils to remove carbonates prior to total organic carbon or CARBON-13 isotopic analysis. *Soil Science Society of America Journal 65*, 1853–1856.

Hatté, C. & Guiot, J. 2005: Palaeoprecipitation reconstruction by inverse modelling using the isotopic signal of loess organic matter: application to the Nußloch loess sequence (Rhine Valley, Germany). *Climate Dynamics 25*, 315–327.

Hatté, C., Antoine, P., Fontugne, M., Lang, A., Rousseau, D.-D. & Zöller, L. 2001: $\delta^{13}C$ of loess organic matter as a potential proxy for paleoprecipitation. *Quaternary Research 55*, 33–38.

Hatté, C., Antoine, P., Fontugne, M., Rousseau, D.-D., Tisnérat-Laborde, N. & Zöller, L. 1999: New chronology and organic matter $\delta^{13}C$ paleoclimatic significance of Nußloch loess sequence (Rhine Valley, Germany). *Quaternary International 62*, 85–91.

Hatté, C., Fontugne, M., Rousseau, D.-D., Antoine, P., Zöller, L., Tisnérat-Laborde, N. & Bentaleb, I. 1998: $\delta^{13}C$ variations of loess organic matter as a record of the vegetation response to climatic changes during the Weichselian. *Geology 26*, 583–586.

Hatté, C., Gauthier, C., Rousseau, D.-D., Antoine, P., Fuchs, M., Lagroix, F., Marković, S. B., Moine, O. & Sima, A. 2013: Excursions to C_4 vegetation recorded in the Upper Pleistocene loess of Surduk (Northern Serbia): an organic isotope geochemistry study. *Climate of the Past 9*, 1001–1014.

Hauck, T. C., Lehmkuhl, F., Zeeden, C., Bösken, J., Thiemann, A. & Richter, J. 2017: The Aurignacian way of life: contextualizing early modern human adaptation in the Carpathian Basin. *Quaternary International 485*, 150–166.

Heller, F. & Tungsheng, L. 1986: Palaeoclimatic and sedimentary history from magnetic susceptibility of loess in China. *Geophysical Research Letters 13*, 1169–1172.

hidmet.gov.rs. 2019: *30 year averages for climate stations in Serbia*. http://www.hidmet.gov.rs/eng/meteorologija/klimatologija_srednjaci.php.

Horváth, F. 1993: Towards a mechanical model for the formation of the Pannonian Basin. *Tectonophysics 226*, 333–357.

Houlton, B. Z., Sigman, D. M., Schuur, E. A. G. & Hedin, L. O. 2007: A climate-driven switch in plant nitrogen acquisition within tropical forest communities. *Proceedings of the National Academy of Sciences 104*, 8902–8906.

Jenny, H. 1941. *Factors of Soil Formation: A System of Quantitative Pedology*. 281 pp. McGraw-Hill, New York.

Jia, G., Rao, Z., Zhang, J., Li, Z. & Chen, F. 2013: Tetraether biomarker records from a loess-paleosol sequence in the western Chinese Loess Plateau. *Frontiers in Microbiology 4*, 199, https://doi.org/10.3389/fmicb.2013.00199.

Jiang, W., Wu, J., Wu, H., Li, Q., Lin, Y. & Yu, Y. 2019: Evolution of the relative abundance of C_4 plants on the Chinese Loess Plateau since the Last Glacial Maximum and its implications. *Journal of Quaternary Science 34*, 101–111.

Jouzel, J., Barkov, N. I., Barnola, J. M., Bender, M., Chapellaz, J., Genthon, C., Kotlyakov, V. M., Lipenkov, V., Lorius, C., Petit, J. R., Raynaud, D., Raisbeck, G., Ritz, C., Sowers, T., Stievenard, M., Yiou, F. & Yiou, P. 1993: Extending the Vostok ice-core record of palaeoclimate to the penultimate glacial period. *Nature 364*, 407–412.

Kaakinen, A., Sonninen, E. & Lunkka, J. P. 2006: Stable isotope record in paleosol carbonates from the Chinese Loess Plateau: implications for late Neogene paleoclimate and paleovegetation. *Palaeogeography, Palaeoclimatology, Palaeoecology 237*, 359–369.

Karger, D. N., Conrad, O., Böhner, J., Kawohl, T., Kreft, H., Soria-Auza, R. W., Zimmermann, N. E., Linder, H. P. & Kessler, M. 2017: Climatologies at high resolution for the earth's land surface areas. *Scientific Data 4*, 170122, https://doi.org/10.1038/sdata.2017.122.

Kawamura, K., Parrenin, F., Lisiecki, L., Uemura, R., Vimeux, F., Severinghaus, J. P., Hutterli, M. A., Nakazawa, T., Aoki, S., Jouzel, J., Raymo, M. E., Matsumoto, K., Nakata, H., Motoyama, H., Fujita, S., Goto-Azuma, K., Fujii, Y. & Watanabe, O. 2007: Northern Hemisphere forcing of climatic cycles in Antarctica over the past 360,000 years. *Nature 448*, 912–916.

Kázmér, M. 1990: Birth, life and death of the Pannonian Lake. *Palaeogeography, Palaeoclimatology, Palaeoecology 79*, 171–188.

Kiss, T., Sipos, G., Mauz, B. & Mezősi, G. 2012: Holocene aeolian sand mobilization, vegetation history and human impact on the stabilized sand dune area of the southern Nyírség, Hungary. *Quaternary Research 78*, 492–501.

Kühn, P., Techmer, A. & Weidenfeller, M. 2013: Lower to middle Weichselian pedogenesis and palaeoclimate in Central Europe using combined micromorphology and geochemistry: the loess-paleosol sequence of Alsheim (Mainz Basin, Germany). *Quaternary Science Reviews 75*, 43–58.

Larson, T. E., Heikoop, J. M., Perkins, G., Chipera, S. J. & Hess, M. A. 2008: Pretreatment technique for siderite removal for organic carbon isotope and C: N ratio analysis in geological samples. *Rapid Communications in Mass Spectrometry 22*, 865–872.

Lehmkuhl, F., Bösken, J., Hošek, J., Sprafke, T., Marković, S. B., Obreht, I., Hambach, U., Sümegi, P., Thiemann, A., Steffens, S., Lindner, H., Veres, D. & Zeeden, C. 2018: Loess distribution and related quaternary sediments in the Carpathian Basin. *Journal of Maps 14*, 661–670.

Leuenberger, M., Siegenthaler, U. & Langway, C. 1992: Carbon isotope composition of atmospheric CO_2 during the last ice age from an Antarctic ice core. *Nature 357*, 488–490.

Lin, B., Liu, R. & An, Z. 1991: Preliminary research on stable isotope composition of Chinese loess. *In* Tunghsheng, L. (eds.): *Loess, Environment and Global Change*, 123–131. Science Press, Beijing.

Liu, J. & Liu, W. 2017: Soil nitrogen isotopic composition of the Xifeng loess-paleosol sequence and its potential for use as a paleoenvironmental proxy. *Quaternary International 440*, 35–41.

Liu, W., Xiahong, F., Youfeng, N., Qingle, Z., Yunning, C. & Zhisheng, A. N. 2005: $\delta^{13}C$ variation of C_3 and C_4 plants across an Asian monsoon rainfall gradient in arid northwestern China. *Global Change Biology 11*, 1094–1100.

Liu, W., Yang, H., Ning, Y. & Zhisheng, A. N. 2007: Contribution of inherent organic carbon to the bulk $\delta^{13}C$ signal in loess deposits from the arid western Chinese Loess Plateau. *Organic Geochemistry 38*, 1571–1579.

Lóczy, D. 2008: The Danube: morphology, evolution and environmental issues. *In* Gupta, A. (ed.): *Large Rivers: Geomorphology and Management*, 235–260. Wiley, Chichester.

Ložek, V. 2001: Molluscan fauna from the loess series of Bohemia and Moravia. *Quaternary International 76–77*, 141–156.

Lu, H. & An, Z. 1998: Paleoclimatic significance of grain size of loess-palaeosol deposit in Chinese Loess Plateau. *Science in China Series D: Earth Sciences 41*, 626–631.

Marino, B. D., McElroy, M. B., Salawitch, R. J. & Spaulding, W. G. 1992: Glacial-to-interglacial variations in the carbon isotopic composition of atmospheric CO_2. *Nature 357*, 461–466.

Marković, S. B., Bokhorst, M. P., Vandenberghe, J., McCoy, W. D., Oches, E. A., Hambach, U., Gaudenyi, T., Jovanović, M., Zöller, L., Stevens, T. & Machalett, B. 2008: Late Pleistocene loess-palaeosol sequences in the Vojvodina Region, north Serbia. *Journal of Quaternary Science 23*, 73–84.

Marković, S. B., Fitzsimmons, K. E., Sprafke, T., Gavrilović, D., Smalley, I. J., Jović, V., Svirčev, Z., Gavrilov, M. B. & Bešlin, M. 2016: The history of Danube loess research. *Quaternary International 399*, 86–99.

Marković, S. B., Hambach, U., Stevens, T., Jovanović, M., O'Hara-Dhand, K., Basarin, B., Lu, H., Smalley, I. J., Buggle, B., Zech, M., Svirčev, Z., Sümegi, P., Milojković, N. & Zöller, L. 2012: Loess in the Vojvodina region (Northern Serbia): an essential link between European and Asian Pleistocene environments. *Netherlands Journal of Geosciences 91*, 173–188.

Marković, S. B., Hambach, U., Stevens, T., Kukla, G. J., Heller, F., McCoy, W. D., Oches, E. A., Buggle, B. & Zöller, L. 2011: The last million years recorded at the Stari Slankamen (Northern Serbia) loess-palaeosol sequencer: revised chronostratigraphy and long-term environmental trends. *Quaternary Science Reviews 30*, 1142–1154.

Marković, S. B., McCoy, W. D., Oches, E. A., Savić, S., Gaudenyi, T., Jovanović, M., Stevens, T., Walther, R., Ivanišević, P. & Garić, Z. 2005: Paleoclimate record in the Upper Pleistocene loess-paleosol sequence at Petrovaradin brickyard (Vojvodina, Serbia). *Geologica Carpathica 56*, 545–552.

Marković, S. B., Oches, E. A., McCoy, W. D., Frechen, M. & Gaudenyi, T. 2007: Malacological and sedimentological evidence for "warm" glacial climate from the Irig loess sequence, Vojvodina, Serbia. *Geochemistry, Geophysics, Geosystems 8*, Q09008, https://doi.org/10.1029/2006gc001565.

Marković, S. B., Oches, E., Sümegi, P., Jovanović, M. & Gaudenyi, T. 2006: An introduction to the Middle and Upper Pleistocene loess–paleosol sequence at Ruma Brickyard, Vojvodina, Serbia. *Quaternary International 149*, 80–86.

Marković, S. B., Stevens, T., Kukla, G. J., Hambach, U., Fitzsimmons, K. E., Gibbard, P., Buggle, B., Zech, M., Guo, Z., Hao, Q., Wu, H., O'Hara-Dhand, K., Smalley, I. J., Újvári, G., Sümegi, P., Timar-Gabor, A., Veres, D., Sirocko, F., Vasiljević, D. A., Jary, Z., Svensson, A., Jović, V., Lehmkuhl, F., Kovács, J. & Svirčev, Z. 2015: Danube loess stratigraphy — Towards a pan-European loess stratigraphic model. *Earth-Science Reviews 148*, 228–258.

Marković, S. B., Sümegi, P., Stevens, T., Schaetzl, R. J., Obreht, I., Chu, W., Buggle, B., Zech, M., Zech, R., Zeeden, C., Gavrilov, M. B., Perić, Z., Svirčev, Z. & Lehmkuhl, F. 2018: The Crvenka loess-paleosol sequence: a record of continuous grassland domination in the southern Carpathian Basin during the Late Pleistocene. *Palaeogeography, Palaeoclimatology, Palaeoecology 509*, 33–46.

Midwood, A. J. & Boutton, T. W. 1998: Soil carbonate decomposition by acid has little effect on $\delta^{13}C$ of organic matter. *Soil Biology and Biochemistry 30*, 1301–1307.

Miklánek, P. 2012: Rivers. *In* Lóczy, D., Stankoviansky, M. & Kotarba, A. (eds.): *Recent Landform Evolution: The Carpatho-Bakan-Dinaric Region*, 31–38. Springer Science & Business Media, Dordrecht.

Miklós, D. & Neppel, F. 2010: Palaeogeography of the Danube and its catchment. *In* Brilly, M. (ed.): *Hydrological Processes of the Danube River Basin*, 79–124. Springer Netherlands, Dordrecht.

Muhs, D. R. 2013: The geologic records of dust in the Quaternary. *Aeolian Research 9*, 3–48.

Muhs, D. R., Aleinikoff, J. N., Stafford, T. W., Kihl, R., Been, J., Mahan, S. A. & Cowherd, S. 1999: Late Quaternary loess in northeastern Colorado: part I - age and paleoclimatic significance. *GSA Bulletin*, *111*, 1861–1875.

Nordt, L. C., Hallmark, C. T., Wilding, L. P. & Boutton, T. W. 1998: Quantifying pedogenic carbonate accumulations using stable carbon isotopes. *Geoderma 82*, 115–136.

Obreht, I., Buggle, B., Catto, N., Marković, S. B., Bösel, S., Vandenberghe, D. A. G., Hambach, U., Svirčev, Z., Lehmkuhl, F., Basarin, B., Gavrilov, M. B. & Jovic, G. 2014: The Late Pleistocene Belotinac section (southern Serbia) at the southern limit of the European loess belt: environmental and climate reconstruction using grain size and stable C and N isotopes. *Quaternary International*, *334–335*, 10–19.

Obreht, I., Hambach, U., Veres, D., Zeeden, C., Bösken, J., Stevens, T., Marković, S. B., Klasen, N.-, Brill, D., Burow, C. & Lehmkuhl, F. 2017: Shift of large-scale atmospheric systems over Europe during late MIS 3 and implications for Modern Human dispersal. *Scientific Reports 7*, 5848, https://doi.org/10.1038/s41598-017-06285-x.

Obreht, I., Zeeden, C., Hambach, U., Veres, D., Marković, S. B. & Lehmkuhl, F. 2019: A critical reevaluation of palaeoclimate proxy records from loess in the Carpathian Basin. *Earth-Science Reviews 190*, 498–520.

Obreht, I., Zeeden, C., Schulte, P., Hambach, U., Eckmeier, E., Timar-Gabor, A. & Lehmkuhl, F. 2015: Aeolian dynamics at the Orlovat loess-paleosol sequence, northern Serbia, based on detailed textural and geochemical evidence. *Aeolian Research 18*, 69–81.

O'Leary, M. H. 1981: Carbon isotope fractionation in plants. *Phytochemistry 20*, 553–567.

O'Leary, M. H. 1988: Carbon isotopes in photosynthesis – fractionation techniques may reveal new aspects of carbon dynamics in plants. *BioScience 38*, 328–336.

Pécsi, M. 1990: Loess is not just the accumulation of dust. *Quaternary International 7*, 1–21.

Pécsi, M. & Richter, G. 1996: Löss - Herkunft - Gliederung - Landschaften. *Zeitschrift für Geomorphologie, Supplementary Issues 98*, 391 pp.

Petit, J. R., Jouzel, J., Raynaud, D., Barkov, N. I., Barnola, J.-M., Basile, I., Bender, M., Chapellaz, J., Davis, M., Delaygue, G., Delmotte, M., Kotlyakov, V. M., Legrand, M., Lipenkov, V. Y., Lorius, C., Pépin, L., Ritz, C., Saltzmann, E. & Stievenard, M. 1999: Climate and atmospheric history of the past 420,000 years from the Vostok ice core, Antarctica. *Nature 399*, 429–436.

Post, W. M., Pastor, J., Zinke, P. J. & Stangenberger, A. G. 1985: Global patterns of soil nitrogen storage. *Nature 317*, 613–616.

Prud'homme, C., Lécuyer, C., Antoine, P., Hatté, C., Moine, O., Fourel, F., Amiot, R., Martineau, F. & Rousseau, D.-D. 2018: $\delta^{13}C$ signal of earthworm calcite granules: a new proxy for palaeoprecipitation reconstructions during the Last Glacial in western Europe. *Quaternary Science Reviews 179*, 158–166.

Prud'homme, C., Lécuyer, C., Antoine, P., Moine, O., Hatté, C., Fourel, F., Martineau, F. & Rousseau, D.-D. 2016: Palaeotemperature reconstruction during the last glacial from $\delta^{18}O$ of earthworm calcite granules from Nussloch loess sequence, Germany. *Earth and Planetary Science Letters 442*, 13–20.

Pustovoytov, K. & Terhorst, B. 2004: An isotopic study of a late Quaternary loess-paleosol sequence in SW Germany. *Revista Mexicana de Ciencias Geológicas 21*, 88–93.

Rao, Z., Xu, Y., Xia, D., Xie, L. & Chen, F. 2013: Variation and paleoclimatic significance of organic carbon isotopes of Ili loess in arid Central Asia. *Organic Geochemistry 63*, 56–63.

Rao, Z., Zhu, Z., Chen, F. & Zhang, J. 2006: Does $\delta^{13}C_{carb}$ of the Chinese loess indicate past C_3/C_4 abundance? A review of research on stable carbon isotopes of the Chinese loess. *Quaternary Science Reviews 25*, 2251–2257.

Robinson, D. 2001: $\delta^{15}N$ as an integrator of the nitrogen cycle. *Trends in Ecology and Evolution 3*, 153–162.

Rousseau, D.-D., Chauvel, C., Sima, A., Hatté, C., Lagroix, F., Antoine, P., Balkanski, Y., Fuchs, M., Mellett, C., Kageyama, M., Ramstein, G. & Lang, A. 2014: European glacial dust deposits: geochemical constraints on atmospheric dust cycle modeling. *Geophysical Research Letters 41*, 7666–7674.

Ruszkiczay-Rüdiger, Z., Fodor, L., Horváth, E. & Telbisz, T. 2009: Discrimination of fluvial, eolian and neotectonic features in a low hilly landscape: a DEM-based morphotectonic analysis in the Central Pannonian Basin, Hungary. *Geomorphology 104*, 203–217.

Schaetzl, R. J., Bettis, E. A., Crouvi, O., Fitzsimmons, K. E., Grimley, D. A., Hambach, U., Lehmkuhl, F., Marković, S. B., Mason, J. A., Owczarek, P., Roberts, H. M., Rousseau, D.-D., Stevens, T., Vandenberghe, J., Zárate, M., Veres, D., Yang, S., Zech, M., Conroy, J. L., Dave, A. K., Faust, D., Hao, Q., Obreht, I., Prud'homme, C., Smalley, I., Tripaldi, A., Zeeden, C. & Zech, R. 2018: Approaches and

challenges to the study of loess—Introduction to the LoessFest Special Issue. *Quaternary Research 89*, 563–618.
Schatz, A.-K., Scholten, T. & Kühn, P. 2015: Paleoclimate and weathering of the Tokaj (Hungary) loess-paleosol sequence. *Palaeogeography, Palaeoclimatology, Palaeoecology 426*, 170–182.
Schatz, A.-K., Zech, M., Buggle, B., Gulyás, S., Hambach, U., Marković, S. B., Sümegi, P. & Scholten, T. 2011: The late Quaternary loess record of Tokaj, Hungary: reconstructing palaeoenvironment, vegetation and climate using stable C and N isotopes and biomarkers. *Quaternary International 240*, 52–61.
Schneider, R., Schmitt, J., Köhler, P., Joos, F. & Fischer, H. 2013: A reconstruction of atmospheric carbon dioxide and its stable carbon isotopic composition from the penultimate glacial maximum to the last glacial inception. *Climate of the Past 9*, 2507–2523.
Schulte, P. & Lehmkuhl, F. 2018: The difference of two laser diffraction patterns as an indicator for post-depositional grain size reduction in loess-paleosol sequences. *Palaeogeography, Palaeoclimatology, Palaeoecology 509*, 126–136.
Schulte, P., Lehmkuhl, F., Kels, H., Loibl, C., Klasen, N. & Hauck, T. 2014: Environmental change indicated by grain-size variations and trace elements: examples from two different sections - the sandy-loess sediments from the Doroshivtsy site (Ukraine) and the loess section Semlac (Romania). *Proscience 1*, 106–112.
Schulte, P., Sprafke, T., Rodrigues, L. & Fitzsimmons, K. E. 2018: Are fixed grain size ratios useful proxies for loess sedimentation dynamics? Experiences from Remizovka, Kazakhstan. *Aeolian Research 31*, 131–140.
Sebe, K., Csillag, G., Ruszkiczay-Rüdiger, Z., Fodor, L., Thamó-Bozsó, E., Müller, P. & Braucher, R. 2011: Wind erosion under cold climate: a Pleistocene periglacial mega-yardang system in Central Europe (Western Pannonian Basin, Hungary). *Geomorphology 134*, 470–482.
Sebe, K., Roetzel, R., Fiebig, M. & Lüthgens, C. 2015: Pleistocene wind system in eastern Austria and its impact on landscape evolution. *Catena 134*, 59–74.
Smalley, I. J. & Leach, J. A. 1978: The origin and distribution of the loess in the Danube Basin and associated regions of East-Central Europe — a review. *Sedimentary Geology 21*, 1–26.
Smalley, I. J., O'Hara-Dhand, K., Wint, J., Machalett, B., Jary, Z. & Jefferson, J. 2009: Rivers and loess: the significance of long river transportation in the complex event-sequence approach to loess deposit formation. *Quaternary International 198*, 7–18.
Sprafke, T. 2016: *Loess in Lower Austria - Archive of Quaternary Climate and Landscape Development*. 273 pp. Würzburg University Press, Würzburg (in German).
Sprafke, T. & Obreht, I. 2016: Loess: rock, sediment or soil – What is missing for its definition? *Quaternary International 399*, 198–207.
Staubwasser, M., Drăguşin, V., Onac, B. P., Assonov, S., Ersek, V., Hoffmann, D. L. & Veres, D. 2018: Impact of climate change on the transition of Neanderthals to modern humans in Europe. *Proceedings of the National Academy of Sciences 115*, 9116–9121.
Stevenson, B. A., Kelly, E. F., McDonald, E. V. & Busacca, A. J. 2005: The stable carbon isotope composition of soil organic carbon and pedogenic carbonates along a bioclimatic gradient in the Palouse region, Washington State, USA. *Geoderma 124*, 37–47.
Sümegi, P., Gulyás, S., Persaits, G., GergelyPáll, D. & Molnár, D. 2011: The loess-paleosol sequence of Basaharc (Hungary) revisited: mollusc-based paleoecological results for the Middle and Upper Pleistocene. *Quaternary International 240*, 181–192.
Szpak, P. 2014: Complexities of nitrogen isotope biogeochemistry in plant-soil systems: implications for the study of ancient agricultural and animal management practices. *Frontiers in Plant Science 5*, 288, https://doi.org/10.3389/fpls.2014.00288.
Terwilliger, V. J., Eshetu, Z., Colman, A., Bekele, T., Gezahgne, A. & Fogel, M. L. 2008: Reconstructing palaeoenvironment from $\delta^{13}C$ and $\delta^{15}N$ values of soil organic matter: a calibration from arid and wetter elevation transects in Ethiopia. *Geoderma 147*, 197–210.
Torre, G., Gaiero, D. M., Cosentino, N. J. & Coppo, R. 2020: The paleoclimatic message from the polymodal grain-size distribution of Late Pleistocene-Early Holocene Pampean loess (Argentina). *Aeolian Research 42*, 100563, https://doi.org/10.1016/j.aeolia.2019.100563.
Tungsheng, L., Zhengtang, G., Naiqin, W. & Huoyuan, L. 1996: Prehistoric vegetation on the Loess Plateau: steppe or forest? *Journal of Southeast Asian Earth Sciences 13*, 341–346.
Vandenberghe, J., Marković, S. B., Jovanović, M. & Hambach, U. 2014: Site-specific variability of loess and palaeosols (Ruma, Vojvodina, northern Serbia). *Quaternary International 334–335*, 86–93.
Varga, Z. 2010: Extra-mediterranean refugia, post-glacial vegetation history and area dynamics in Eastern Central Europe. *In* Habel, J. C. & Assmann, T. (eds.): *Relict Species*, 57–87. Springer, Berlin.
Vidic, N. J. & Montañez, I. P. 2004: Climatically driven glacial-interglacial variations in C_3 and C_4 plant proportions on the Chinese Loess Plateau. *Geology 32*, 337–340.
Vinnepand, M., Fischer, P., Fitzsimmons, K. E., Thornton, B., Fiedler, S. & Vött, A. 2020: Combining inorganic and organic carbon stable isotope signatures in the Schwalbenberg loess-palaeosol-sequence near Remagen (Middle Rhine Valley, Germany). *Frontiers in Earth Science 8*, 276, https://doi.org/10.3389/feart.2020.00276.
Vuillemin, A., Friese, A., Wirth, R., Schuessler, J. A., Schleicher, A. M., Kemnitz, H., Lücke, A., Bauer, K. W., Nomosatryo, S., von Blanckenburg, F., Simister, R., Ordoñez, L. G., Ariztegui, D., Henny, C., Russell, J. M., Bijaksana, S., Vogel, H., Crowe, S. A., Kallmeyer, J. & the Towuti Drilling Project Science team 2020: Vivianite formation in ferruginous sediments from Lake Towuti, Indonesia. *Biogeosciences 17*, 1955–1973.
Wang, H., Ambrose, S. H., Liu, C.-L. J. & Follmer, L. R. 1997: Paleosol stable isotope evidence for Early Hominid occupation of East Asian temperate environments. *Quaternary Research 48*, 228–238.
Weiguo, L., Xiahong, F., Youfeng, N., Qingle, Z., Yunning, C. & Zhisheng, A. N. 2005: $\delta^{13}C$ variation of C_3 and C_4 plants across an Asian monsoon rainfall gradient in arid northwestern China. *Global Change Biology 11*, 1094–1100.
Wielstra, B., Crnobrnja-Isailović, J., Litvinchuk, S. N., Reijnen, B. T., Skidmore, A. K., Sotiropoulos, K., Toxopeus, A. G., Tzankov, N., Vukoc, T. & Arntzen, J. W. 2013: Tracing glacial refugia of Triturus newts based on mitochondrial DNA phylogeography and species distribution modeling. *Frontiers in Zoology 10*, 13, https://doi.org/10.1186/1742-9994-10-13.
Willis, K. J., Rudner, E. & Sümegi, P. 2000: The full-glacial forests of Central and Southeastern Europe. *Quaternary Research 53*, 203–213.
Wooller, M. J., Zazula, G. D., Edwards, M., Froese, D. G., Boone, R. D., Parker, C. & Bennett, B. 2007: Stable carbon isotope compositions of eastern Beringian grasses and sedges: investigating their potential as paleoenvironmental indicators. *Arctic, Antarctic, and Alpine Research 39*, 318–331.
Xie, S., Guo, J., Huang, J., Chen, F., Wang, H. & Farrimond, P. 2004: Restricted utility of $\delta^{13}C$ of bulk organic matter as a record of paleovegetation in some loess-paleosol sequences in the Chinese Loess Plateau. *Quaternary Research 62*, 86–93.
Yang, S. & Ding, Z. 2006: Winter–spring precipitation as the principal control on predominance of C3 plants in Central Asia over the past 1.77 Myr: evidence from $\delta^{13}C$ of loess organic matter in Tajikistan. *Palaeogeography, Palaeoclimatology, Palaeoecology 235*, 330–339.
Youfeng, N., Weiguo, L. & Zhisheng, A. 2008: A 130-ka reconstruction of precipitation on the Chinese Loess Plateau from organic carbon isotopes. *Palaeogeography, Palaeoclimatology, Palaeoecology 270*, 59–63.
Zech, M., Bimüller, C., Hemp, A., Samimi, C., Broesike, C., Hörold, C. & Zech, W. 2011: Human and climate impact on ^{15}N natural abundance of plants and soils in high-mountain ecosystems: a short review and two examples from the Eastern Pamirs and Mt. Kilimanjaro. *Isotopes in Environmental and Health Studies 47*, 286–296.
Zech, M., Buggle, B., Leiber, K., Marković, S. B., Glaser, B., Hambach, U., Huwe, B., Stevens, T., Sümegi, P., Wiesenberg, G. & Zöller, L. 2010: Reconstructing Quaternary vegetation history in the Carpathian Basin, SE-Europe, using n-alkane biomarkers as molecular fossils: problems and possible solutions, potential and limitations. *E&G Quaternary Science Journal 58*, 145–155.

Zech, M., Zech, R. & Glaser, B. 2007: A 240,000-year stable carbon and nitrogen isotope record from a loess-like palaeosol sequence in the Tumara Valley, Northeast Siberia. *Chemical Geology 242*, 307–318.
Zech, R., Zech, M., Marković, S. B., Hambach, U. & Huang, Y. 2013: Humid glacials, arid interglacials? Critical thoughts on pedogenesis and paleoclimate based on multi-proxy analyses of the loess–paleosol sequence Crvenka, Northern Serbia. *Palaeogeography, Palaeoclimatology, Palaeoecology 387*, 165–175.
Zeeden, C., Kels, H., Hambach, U., Schulte, P., Protze, J., Eckmeier, E., Marković, S. B., Klasen, N. & Lehmkuhl, F. 2016: Three climatic cycles recorded in a loess-palaeosol sequence at Semlac (Romania) – Implications for dust accumulation in south-eastern Europe. *Quaternary Science Reviews 154*, 130–142.
Zhou, L., Song, M.-H., Wang, S.-Q., Fan, J.-W., Liu, J.-Y., Zhong, H.-P., Yu, G.-R., Gao, L.-P., Hu, Z.-M., Chen, B., Wu, W.-X. & Song, T. 2014: Patterns of soil ^{15}N and total N and their relationships with environmental factors on the Qinghai-Tibetan Plateau. *Pedosphere 24*, 232–242.
Zöller, L. 2010: New approaches to European loess: a stratigraphic and methodical review of the past decade. *Open Geosciences 2*, 19–31.

Supporting Information

Additional Supporting Information may be found in the online version of this article at http://www.boreas.dk.

Fig. S1. $\delta^{13}C_{org}$ compositions after fumigation treatment (FM_{IR}, *x*-axis) and wet chemical treatment for 4 h (WC_{IR} 4 h, *y*-axis) of the samples from Irig.

Fig. S2. $\delta^{13}C_{org}$ compositions after wet chemical treatment for 2 (WC_{SE} 2 h, *x*-axis) and 4 h (WC_{SE} 4 h, *y*-axis) of the samples from Semlac.

Fig. S3. C/N ratios and $\delta^{13}C_{org}$ compositions for test sample set from Irig after fumigation method (A) and (B), and wet chemical acidification for 4 h (C and D).

Table S1. Used calibration standards for isotope ratio measurements, their isotopic composition and standard deviations (SD).

Table S2. Mean values for C/N, $\delta^{13}C_{org}$ and $\delta^{15}N$ for the stratigraphical units for Semlac and Irig.

Table S3. *F*-test for the mean values of the C/N ratio for the stratigraphical units for Semlac and Irig (significance level $\alpha = 0.05$).

Table S4. *F*-test for the mean values of the $\delta^{13}C_{org}$ ratio for the stratigraphical units for Semlac and Irig (significance level $\alpha = 0.05$).

Table S5. *F*-test for the mean values of the $\delta^{15}N$ ratio for the stratigraphical units for Semlac and Irig (significance level $\alpha = 0.05$).

Table S6. Student's *t*-test for the mean values of the C/N ratio for the stratigraphical units for Semlac and Irig (significance level $\alpha = 0.05$).

Table S7. Student's *t*-test for the mean values of the $\delta^{13}C_{org}$ ratio for the stratigraphical units for Semlac and Irig (significance level $\alpha = 0.05$).

Table S8. Student's *t*-test for the mean values of the $\delta^{15}N$ ratio for the stratigraphical units for Semlac and Irig (significance level $\alpha = 0.05$).